ADVANCED MATERIALS
www.advmat.de

A New Frontier of Printed Electronics: Flexible Hybrid Electronics

Yasser Khan, Arno Thielens, Sifat Muin, Jonathan Ting, Carol Baumbauer, and Ana C. Arias**

The performance and integration density of silicon integrated circuits (ICs) have progressed at an unprecedented pace in the past 60 years. While silicon ICs thrive at low-power high-performance computing, creating flexible and large-area electronics using silicon remains a challenge. On the other hand, flexible and printed electronics use intrinsically flexible materials and printing techniques to manufacture compliant and large-area electronics. Nonetheless, flexible electronics are not as efficient as silicon ICs for computation and signal communication. Flexible hybrid electronics (FHE) leverages the strengths of these two dissimilar technologies. It uses flexible and printed electronics where flexibility and scalability are required, i.e., for sensing and actuating, and silicon ICs for computation and communication purposes. Combining flexible electronics and silicon ICs yields a very powerful and versatile technology with a vast range of applications. Here, the fundamental building blocks of an FHE system, printed sensors and circuits, thinned silicon ICs, printed antennas, printed energy harvesting and storage modules, and printed displays, are discussed. Emerging application areas of FHE in wearable health, structural health, industrial, environmental, and agricultural sensing are reviewed. Overall, the recent progress, fabrication, application, and challenges, and an outlook, related to FHE are presented.

1. Introduction

In recent years, form factors of electronics have started to change from their traditional rigid and rectangular shapes to more complex form factors—soft, flexible, bendable, and stretchable.[1–4] These next-generation electronics are lightweight and conform to the curves of the body or bend around structures and objects. Researchers are using these new forms of electronics to interface with biology and nature.[5–10] With advanced printing techniques, these nontraditional electronics can be manufactured in large areas—in the kilometers scale.[11–18] Although developments of flexible and printed electronics progressed significantly, they present a few major limitations that multiple decades of research have not been able to resolve—high power consumption, low performance and limited lifetime. On the other hand, silicon integrated circuits (ICs) do not suffer from these limitations and provide unparalleled performance at low power consumption for years. Nevertheless, silicon ICs are constrained to their rigid and bulky form factors. In addition, silicon IC manufacturing relies heavily on vacuum deposition that makes large-area scaling challenging and expensive.[17,19–21] Flexible hybrid electronics (FHE) combines silicon ICs to flexible and printed electronics and brings low-power and high-performance computing capabilities in large-area form factors. In essence, FHE is a versatile and powerful electronics platform, which is flexible, efficient, cost-effective, and large-area compliant.

Printing is currently a commercially viable manufacturing technology for fabricating electronics, mainly due to the recent advances in printable metallic,[22,23] insulating,[24,25] and semiconducting materials[26–30] and mature printing techniques.[26,31–36] While initial efforts in printed electronics were directed toward display and lighting industries,[37–39] printed electronics now spans electronic devices,[40,41] sensors,[42–46] and even circuits[47–50] with applications in energy, health, and consumer electronics. In industry and academia, both passive and active electronic devices are manufactured using inkjet printing, screen printing, gravure printing, blade coating, spray coating, and other hybrid printing methods.

Standard silicon microfabrication utilizes blanket material deposition, photolithography, and etch steps for each layer in the device stack. In this subtractive process, vacuum deposition or drop-casting is used for deposition. After photopatterning, the excess material is removed. Therefore, scaling up this subtractive process to large-area is expensive and wasteful. On the other hand, printing is an additive manufacturing process. Selective deposition of solution processable materials reduces cost by eliminating photolithography and etch steps used in microfabrication. Large-area, high-volume, and roll-to-roll manufacturing are major strengths of printed electronics, in addition to the capability of printing devices on soft, flexible, and

Dr. Y. Khan,[+] Dr. A. Thielens, J. Ting, C. Baumbauer, Prof. A. C. Arias
Department of Electrical Engineering and Computer Sciences
University of California
Berkeley, Berkeley, CA 94720, USA
E-mail: yasser.khan@berkeley.edu; acarias@eecs.berkeley.edu
Dr. S. Muin
Department of Civil and Environmental Engineering
University of California
Berkeley, Berkeley, CA 94720, USA

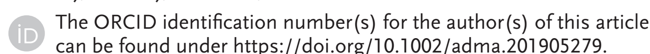
The ORCID identification number(s) for the author(s) of this article can be found under https://doi.org/10.1002/adma.201905279.

[+]Present address: Department of Chemical Engineering, Stanford University, 443 Via Ortega, Stanford, CA 94305-4125, USA

DOI: 10.1002/adma.201905279

 © 2019 WILEY-VCH Verlag GmbH & Co. KGaA, Weinheim

nontraditional substrates. Although progress has been made at a steady pace demonstrating printed organic transistors with carrier mobilities over 1 cm^2 V^{-1} s^{-1}[51] and switching speed in the MHz range,[30] silicon electronics outperforms printed electronics in terms of carrier mobilities and switching speeds in three orders of magnitudes, as shown in **Figure 1**a. However, printed electronics provides unique advantages such as manufacturing on soft substrates in large-areas with high throughput. These qualities are complementary to silicon ICs (Figure 1a).

FHE is a key enabling technology for system-level implementations of nonsilicon electronics.[52–56] Silicon ICs are mature and compatible with existing computation and communication standards. On the other hand, data processing and transmission of flexible electronic systems need to be compatible with existing methods and standards—FHE provides that compatibility bridge. Figure 1b shows a system-level implementation of FHE. The usage of silicon ICs and printed electronics in this system is shown using blue and orange color bars underneath the system blocks. First, printed electronics is used for sensing. Second, printed circuits can also be used for signal conditioning. However, in general, silicon ICs are employed for signal conditioning and processing. Here, both technologies have potential overlapping usage. Finally, the data in a FHE system is displayed using a printed display or transmitted to a remote host.

Breaking away from the rigid form factors of conventional electronics, electronics that flex and wrap around the body, objects, and structures have endless sensing applications. Healthcare is currently the biggest application field for FHE, especially flexible wearable medical devices.[5,57–60] Sensitive and high-performance soft sensors are being developed for bioelectronic, biophotonic, and biochemical sensing in research labs around the world. Soft electronics are lightweight and comfortable to wear, also do not compromise the measurement quality. Application areas for FHE stretch beyond healthcare. Printed and large-area sensor arrays can be used for industrial, environmental, and agricultural sensing.[61–64] Future Internet of things (IoT) infrastructures will require a vast number of sensors that are high-performance and low-cost—FHE is well suited for deploying a massive number of devices. Also, structural health monitoring can benefit from distributed sensing where sensors cover a vast area and provide critical parameters that can be correlated to the health of the structure.[65,66] Apart from civil structures, FHE can be used to monitor the performance and state of cars and airplanes operating in normal and extreme conditions.[67] The ability to deploy sensors on irregular and complex shapes is a fundamental advantage of FHE over existing electronics—sensors can be embedded into expensive machinery and robotic tools to precisely monitor performance and perform early maintenance to avoid mishaps or tool down-times. Overall, FHE systems that are reliable, low-cost, lightweight, flexible, and stretchable have endless applications in medical, industrial, and consumer electronics. IDTechEx, a market research agency, forecasts printed, flexible, and organic electronics will grow to a $73.3 billion industry by 2029 from $31.7 billion in 2019.[68]

Here, we review the materials, methods, and applications of FHE, while discussing the recent progress in the field. In Section 2, we present the core components of FHE: 1) printed sensors and circuits, 2) thinned silicon ICs, 3) printed antennas for power and communications, 4) printed power source and

Yasser Khan is a postdoctoral scholar at Stanford University, advised by Professor Zhenan Bao in chemical engineering and Professor Boris Murmann in electrical engineering. He received his B.S. in electrical engineering from the University of Texas at Dallas in 2010 and his M.S. in electrical engineering from King Abdullah University of Science and Technology in 2012. He completed his Ph.D. in electrical engineering and computer sciences from the University of California, Berkeley in 2018, from Professor Ana Claudia Arias's research group. His research focuses on wearable medical devices, with an emphasis on skin-like soft sensor systems.

Arno Thielens is a postdoctoral researcher at UC Berkeley and Ghent University. He received his M.S. degree and Ph.D. degree in applied physics at Ghent University in 2010 and 2015, respectively. He is affiliated to Ghent University's Waves group as a postdoctoral researcher, where his research focuses on personal exposure assessment to radio-frequency electromagnetic fields and numerical dosimetry. Since 2017, he has also been a member of the Berkeley Wireless Research Center at the University of California, Berkeley, where he is working on antenna design, body area networks, and the development of the human intranet.

Ana C. Arias is a professor of electrical engineering and computer sciences at the University of California, Berkeley. She received her bachelor's and master's degrees from the Federal University of Paraná in Curitiba, Brazil, in 1995 and 1997, respectively, and her Ph.D. degree from the University of Cambridge, U.K., in 2001, all in physics. She was the Manager of the Printed Electronic Devices Area and a member of Research Staff at PARC, a Xerox Company. She went to PARC, in 2003, from Plastic Logic in Cambridge, UK, where she led the semiconductor group. Her research focuses on the use of electronic materials processed from solution in flexible electronic systems. She uses printing techniques to fabricate flexible large-area electronic devices and sensors.

© 2019 WILEY-VCH Verlag GmbH & Co. KGaA, Weinheim

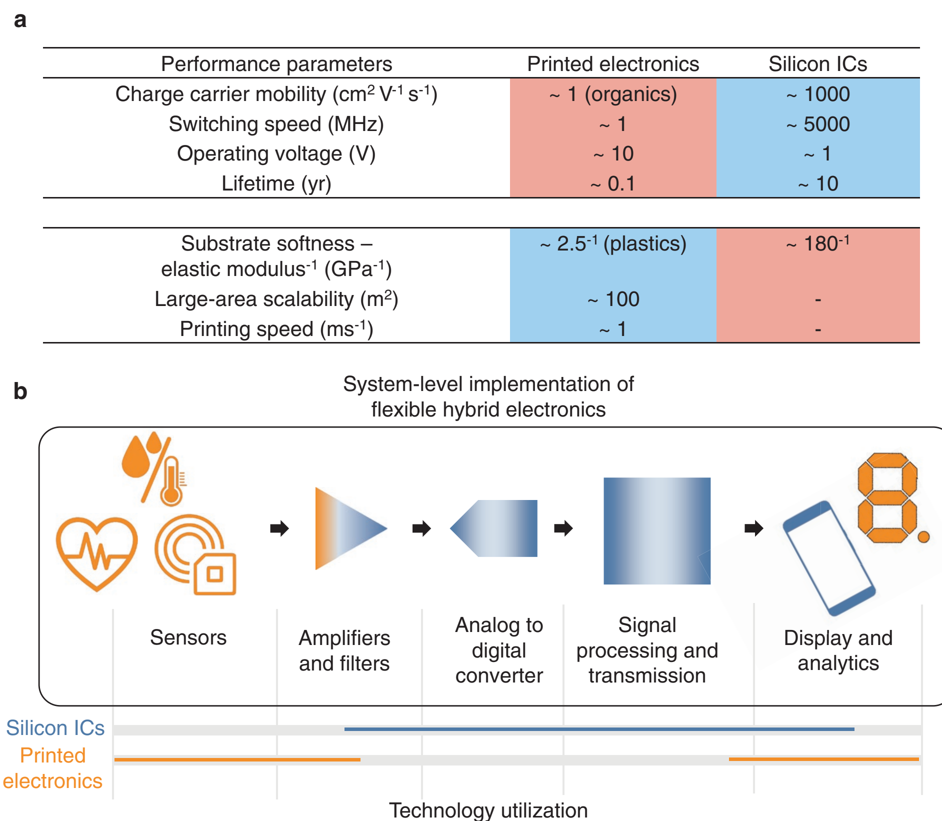

a

Performance parameters	Printed electronics	Silicon ICs
Charge carrier mobility ($cm^2 V^{-1} s^{-1}$)	~ 1 (organics)	~ 1000
Switching speed (MHz)	~ 1	~ 5000
Operating voltage (V)	~ 10	~ 1
Lifetime (yr)	~ 0.1	~ 10
Substrate softness – elastic modulus^{-1} (GPa^{-1})	~ 2.5^{-1} (plastics)	~ 180^{-1}
Large-area scalability (m^2)	~ 100	-
Printing speed (ms^{-1})	~ 1	-

Figure 1. Performance comparison and utilization of printed electronics and silicon ICs in FHE systems. a) Charge-carrier mobility, switching speed, operating voltage, lifetime, substrate softness, large-area scalability, and printing speed comparison between the two technologies. The data are color-coded in light blue (desirable) and red (not desirable) to show the complementary nature of printed electronics and silicon ICs. b) System-level implementation of FHE showing the utilization of both printed electronics and silicon ICs. The color bars under the system blocks show where silicon ICs (blue) and printed electronics (orange) are utilized.

storage modules, and 5) printed displays. The applications of FHE are reviewed in Section 3. FHE for wearable medical devices is presented in Section 3.1. Industrial, environmental, and agricultural monitoring with FHE is discussed in Section 3.2. FHE systems that are applied for structural health monitoring are reviewed in Section 3.3. Finally, reliability testing and challenges in FHE are discussed in Section 4. A visual overview of this review paper is shown in **Figure 2**. Overall, in this review paper, we focus on the fundamental building blocks of FHE, i.e., components of printed electronics and their system-level integration to silicon ICs. While FHE is extensively used for medical applications,[58,60] we explore new directions of FHE in structural health, industrial, environmental, and agricultural sensing, and discuss the limitations and outlook of this powerful technology.

2. Core Components of FHE

FHE systems use printed sensors to transduce physical and chemical quantities such as temperature, light, pressure, chemical concentrations, etc. to electrical signals. That electrical signal is conditioned and processed with silicon ICs, and then, transmitted to an external host with printed antennas or displayed on a printed display. The system is usually powered by a printed battery or by energy harvesters. A simplified FHE system highlighting the core components is shown in **Figure 3**. Here, many printed electronic components and silicon ICs are integrated on a flexible substrate. Generally, printing is the major fabrication technique used in FHE. Therefore, in Section 2.1, we introduce printed electronics and its major parts. We discuss substrates, inks, and different printing techniques, and review sensors and circuits fabricated using printing. Thinned silicon ICs that handle signal computation and communication in FHE, is discussed in Section 2.2. Next, current progress in printed antennas, printed energy harvesting and storage modules, and printed displays are presented in Section 2.3, 2.4, and 2.5, respectively.

2.1. Printed Sensors and Circuits

The rapid advancement in printed electronics in the past two decades encouraged innovations in FHE. Solution processability and large-area scalability are inherent benefits of printed electronics that make it a commercially viable technology. Here, we discuss the components and concepts of printed electronics—substrates, inks, and different printing techniques. Although it is not an exhaustive list of materials and methods, this section is a primer on printed electronics that can be used with FHE.

© 2019 WILEY-VCH Verlag GmbH & Co. KGaA, Weinheim

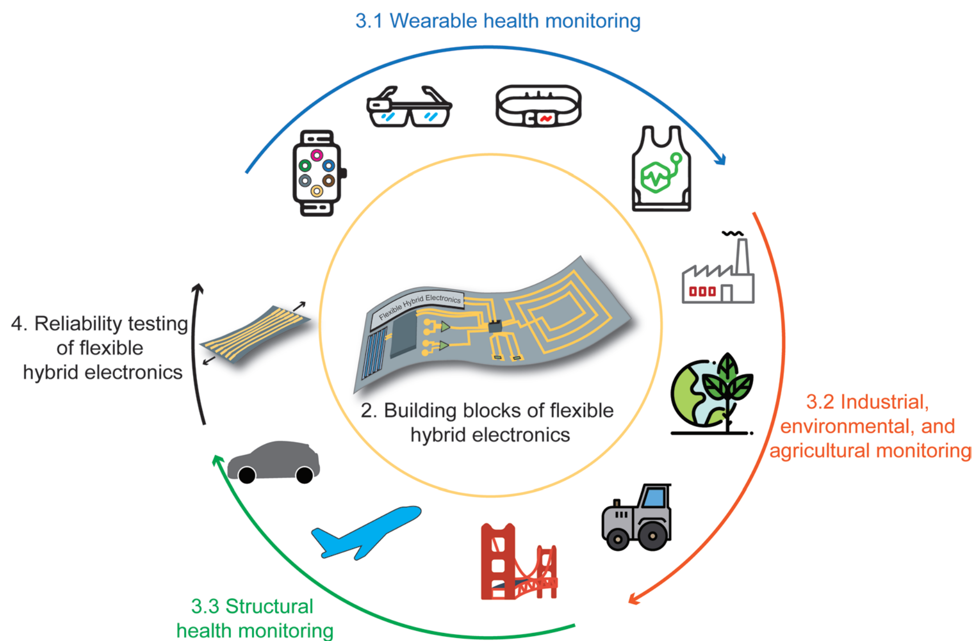

Figure 2. A visual overview of this review paper. Section 2 presents the fundamental building blocks of FHE. Materials and methods for fabricating FHE systems are discussed in this section. Section 3 presents various application areas of FHE. Section 3.1 presents recently reported wearable electronics that use FHE. Section 3.2 discusses industrial, environmental, and agricultural monitoring with FHE. Section 3.3 presents FHE systems that are applied for structural health monitoring. Reliability testing and challenges in FHE are discussed in Section 4.

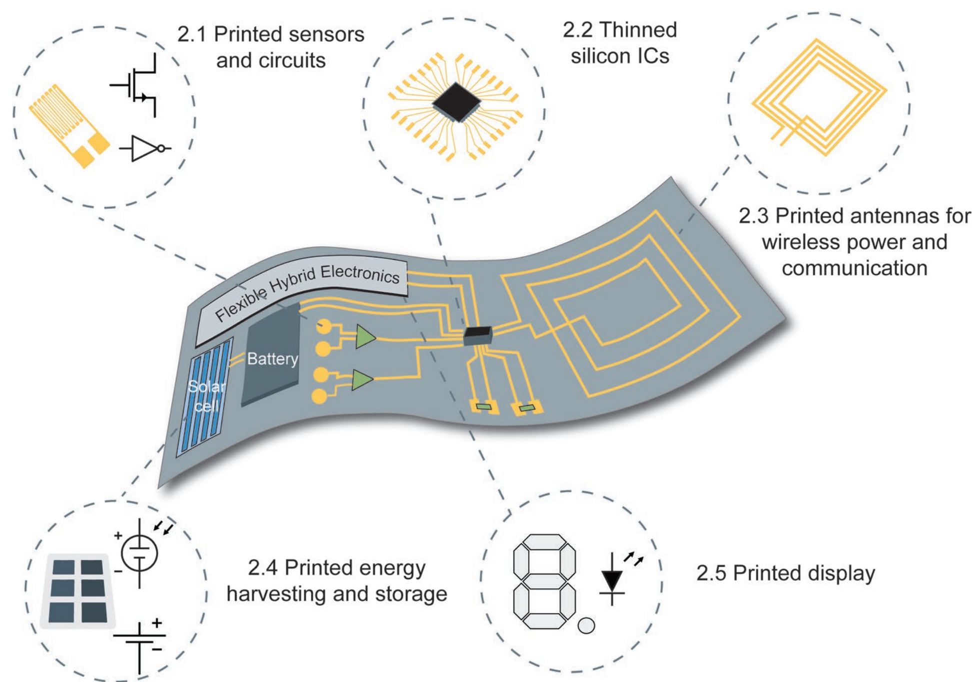

Figure 3. A flexible electronic system, showing the key components of FHE. Various printed sensors and circuits can be used in FHE: in Section 2.1 printed electronics and its major parts are reviewed. Substrates, inks, and different printing techniques, as well as printed sensors and circuits are discussed. At the core of an FHE system, silicon ICs are used for sensor data processing and communication. In Section 2.2, silicon IC interfacing techniques used in FHE are presented. Printed antennas for wireless power and communication are discussed in Section 2.3. Depending on the operation, FHE systems require energy harvesting and storage modules: these are presented in Section 2.4. Recent progress in printed displays, which are also an application-dependent module are presented in Section 2.5.

© 2019 WILEY-VCH Verlag GmbH & Co. KGaA, Weinheim

2.1.1. Substrates

The most common substrates for printed electronics are polyethylene derivatives—poly(ethylene terephthalate) (PET) and polyethylene naphthalate (PEN).[15,23] These substrates are low-cost, optically transparent, come in various thicknesses, and have been widely used in the literature. Besides, their surface roughness can be as low as a few nm with planarization, which makes them suitable for high-performance printed electronics and optoelectronics. One of the biggest limitations of these substrates is a low thermal budget. FHE requires bonding silicon ICs to the printed sensors and circuits, and if solder is used for these connections, a relatively high thermal budget is required.[52–54] Solder reflow temperature can be as high as 204 °C for tin–lead (Sn–Pb) which is above the glass-transition temperature (T_g) of PET and PEN.

There are low-temperature alternatives such as tin–bismuth (Sn–Bi) solder, which has a solder reflow temperature of 175 °C.[54] However, these temperatures are close to the T_g of PET and PEN. On the other hand, Kapton polyimide (PI) has a much higher T_g, making it a good alternative for FHE. Moreover, PI is widely used in the commercial flexible printed circuit board (FPCB) industry. However, Kapton PI is expensive, the surface roughness is high, and the films are opaque. There are other alternatives such as poly(ether–ether–ketone) (PEEK), whose fire-resistant property is useful for wearable devices that need to be nonflammable.[74] However, PEEK has limitations such as high surface roughness and price. Paper can also be used as a substrate for printed electronics. Since paper is fibrous, many layers of planarization are required to use paper as a substrate.[75] Furthermore, elastomers are also becoming popular for fabricating stretchable devices—polydimethylsiloxane (PDMS) is by far the most common substrate for fabricating soft and stretchable electronics.[76] The common substrates in printed electronics and their performance parameters are listed in **Table 1**.

2.1.2. Inks

To print an electronic device three types of inks are required—semiconducting, insulating, and metallic. In a transistor, the device performance parameters such as carrier mobility, threshold voltage, and on/off ratio depend heavily on the semiconductors. Organic semiconductors and metal oxides are used as semiconductors in printed electronics due to their solution processability. Organic semiconductors demonstrate carrier mobility of 1–40 cm^2 V^{-1} s^{-1} for p-type and 0.1–5 cm^2 V^{-1} s^{-1} for n-type materials.[69] Printable metal oxides have higher carrier mobility than organics, 1–100 cm^2 V^{-1} s^{-1}.[77] In comparison, crystalline silicon has an electron mobility of 1500 cm^2 V^{-1} s^{-1}, and hole mobility of 450 cm^2 V^{-1} s^{-1}. Therefore, switching speeds for the best-printed transistors are still in the MHz regime, while crystalline silicon transistors go beyond a few GHz.

Table 1. Substrates for FHE and their physical properties.

Substrate	Thickness [µm]	Transparency [%]	Density [g cm^{-3}]	T_g [°C]	Young's modulus [GPa]	Ref.
PET	16–100	90	1.38	80	2.8	[69]
PEN	12–250	87	1.4	120	3.0	[69]
PI	12–125	–	1.4	410	2.5	[69]
PEEK	12–1500	54	1.32	143	2.6	[70]
Paper	20–250	–	0.6–1.0	–	0.5–3.5	[69,71]
PDMS	5–1500	92	0.965	125	0.57–3.7	[72,73]

Organic dielectrics are great insulating materials as they are transparent, solution-processable, have high dielectric constant $\varepsilon \approx 10$, and provide smooth films on plastic substrates. The most common dielectric materials in printed electronics are poly(vinylpyrrolidone) (PVP), polystyrene (PS), poly(methyl methacrylate) (PMMA), poly(vinyl alcohol) (PVA), poly(vinyl chloride) (PVC), poly(vinylidene fluoride) (PVDF), and amorphous fluoropolymers.[80] All these materials are compatible with different printing techniques.

Metals form the contacts for single electronic elements, and they connect multiple electronic elements in a circuit. Silver, gold, and copper nanoparticle suspensions are widely used in printed electronics for contacts and interconnects. Poly(3,4-ethylenedioxythiophene)–poly(styrenesulfonate) (PEDOT:PSS), carbon nanomaterials, and metallic oxides are also used in printed electronics. Solution-processed low viscosity <100 centipoise (cP) inks are used with several printing techniques for fabricating various electronic devices and sensors. Low-viscosity inks generally result in a smooth and pristine printed film, therefore, they are used to fabricate electronics and optoelectronics such as transistors,[29] electronic circuits,[45] light-emitting diodes,[81,82] photodiodes,[83] and solar cells.[84] On the other hand, high-viscosity inks (1000–100 000 cP) are used mostly for making conductive traces or passive electronic elements.[15]

Another crucial aspect of ink design is ink formulation. Solvents, additives, surfactants, and binders are mixed with pristine semiconducting, insulating, and metallic materials to enhance the printability of functional inks.[85] While designing an ink several considerations are made, namely, reducing the coffee-ring effect, improving wetting on the surface while suppressing ink spreading, long-term ink stability, and compatibility with a given printing technique.[86] Low-viscosity metallic inks can be made with metallic micro- and nanoparticle dispersions, conducting polymer solutions, and nanocarbon material dispersions.[87] These low-viscosity inks without binders enable printing of high-purity materials.[34] In contrast, high-viscosity inks typically are formulated with binders and surfactants. However, to increase conductivity, high-viscosity inks can be printed in a thick layer (hundreds of µm) in comparison to low-viscosity inks with sintered thickness ≈1 µm. As for the insulating and semiconducting inks, solvents are picked considering solubility and printability of the ink. Also, orthogonality is particularly critical when printing a multilayer structure. Solvent orthogonality ensures solvent from one layer does not dissolve the material deposited in another layer using another solvent. Nonorthogonal solvents swell the semiconductor layer and increase their surface roughness, which degrades performance.[25]

A variety of printing techniques can be used to deposit ink on flexible substrates, however, ink viscosity, the surface roughness of the deposited film, patterning requirements should be taken into account to choose the right combination of inks and substrates. Typically, low-viscosity inks are printed using inkjet

© 2019 WILEY-VCH Verlag GmbH & Co. KGaA, Weinheim

printing, gravure printing, blade coating, slot-die coating, or spray coating. On the other hand, high-viscosity inks are printed using screen printing, stencil printing, or microdispense printing.

2.1.3. Printing Techniques

Since FHE utilizes the versatility of low-cost printed electronics, printing methods are an essential for FHE. Digital drop-on-demand printing techniques such as inkjet printing as well as high-volume and roll-to-roll printing methods are currently used to manufacture FHE. The main printing techniques are discussed below.

Inkjet Printing: Inkjet printing is a digital printing process, which is heavily used for prototyping as well as large-volume manufacturing of electronics.[34,88] Usually, the ink reservoirs of inkjet printers are coupled with piezoconstrictors that loads and expels ink based on the applied bias, as shown in the schematic of **Figure 4**a,b. Since each drop can be controlled, ink consumption is extremely low in inkjet printing. Semiconducting, insulating, and metallic low viscosity (5–50 cP) ink can be printed with inkjet. Therefore, smooth and ≈70 µm wide feature size is achievable with 10 pL drops of ink. Figure 4c shows an inkjet-printed electrode array that was fabricated using inkjet printing.[23] The printed patterns are digitally generated and can be changed on-the-fly, which makes inkjet printing a great choice for prototyping. One drawback of inkjet is—it uses a raster motion for printing, which slows down the printing process compared to the roll-to-roll processes.

Screen Printing: Screen printing is a fast, high-volume printing technique. In screen printing, a flood bar spreads the ink over the screen, and a squeegee is used to transfer ink through the screen, as shown in the schematic and the photograph of Figure 4d,e.[78] The mesh screen determines the feature that gets transferred to the substrate. With screen printing it is possible to get thick (≈100 µm) features. However, in general, the deposited film is rough due to the highly viscous (500–5000 cp) nature of the inks used in screen printing. As demonstrated by Ostfeld et al., screen printing is a great choice for printing interconnects and passive circuit elements such as resistors, capacitors, and inductors for FHE (Figure 4f).[15]

Gravure Printing: Gravure printing is the most promising roll-to-roll printing technique as it can produce high-resolution patterns at high speeds (≈10 ms^{-1}). As shown in the schematic

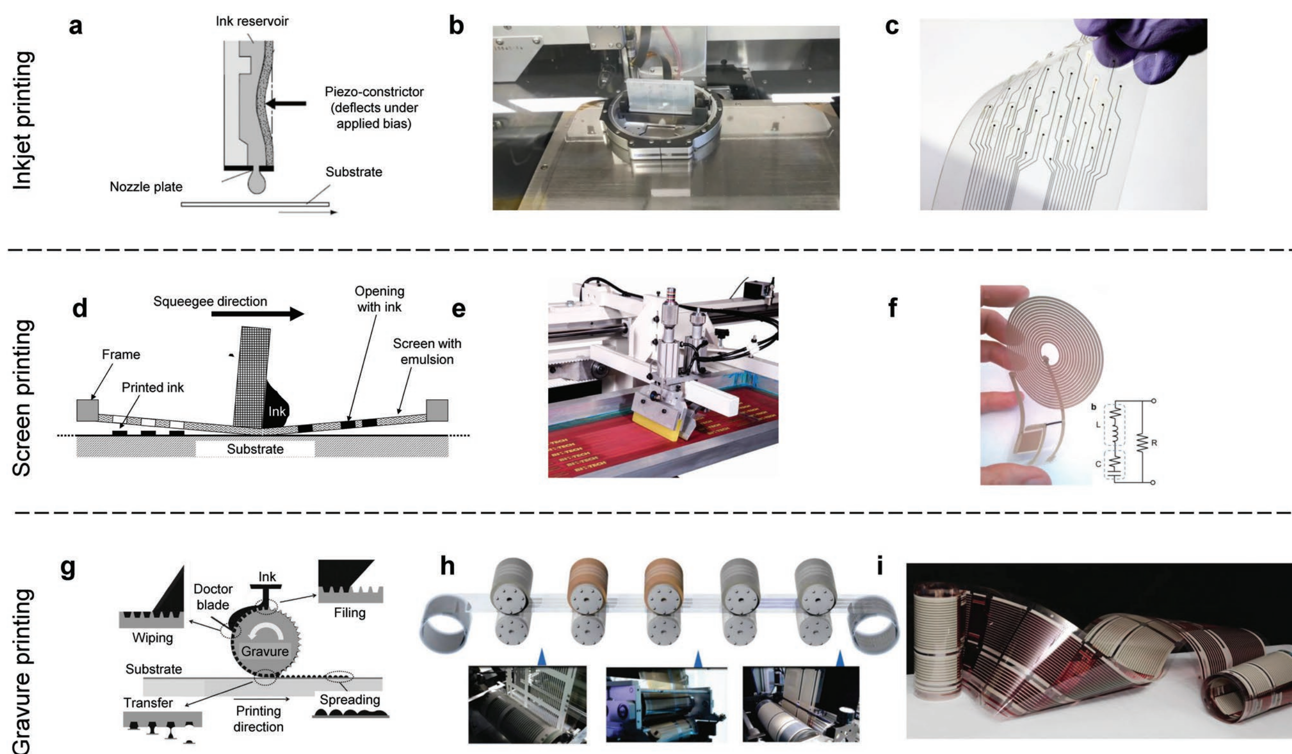

Figure 4. Different printing techniques used in printed electronics. a–c) Schematic, photo, and a device fabricated using inkjet printing, respectively. a) A piezoconstrictor is used to load and expel ink from the reservoir. The voltage waveform and the nozzle size determine the volume of dispensed ink. Reproduced with permission.[34] Copyright 2015, IEEE. b) Photograph showing an inkjet printer head while printing on a plastic substrate. c) An electrode array fabricated using inkjet-printed gold nanoparticles. b,c) Reproduced with permission.[23] Copyright 2016, Wiley-VCH. d–f) Schematic, photo, and a device fabricated using screen printing, respectively. d) A squeegee is used to force ink through a screen. The pattern on the screen gets transferred to the substrate. Reproduced with permission.[78] Copyright 2009, Elsevier. e) A photo of a screen printer while printing with a squeegee. f) An RLC circuit consisting of a resistor, an inductor, and a capacitor fabricated using screen printing. e,f) Reproduced under the terms of the CC-BY Creative Commons Attribution 4.0 International License (http://creativecommons.org/licenses/by/4.0/).[15] Copyright 2015, Springer Nature. g–i) Schematic, photo, and a device fabricated using gravure printing, respectively. g) Schematic showing the different steps of gravure printing. Reproduced with permission.[34] Copyright 2015, IEEE. h) Roll-to-roll gravure printing process of inverted OPV modules. i) Rolls of gravure-printed inverted OPV modules. h,i) Reproduced with permission.[79] Copyright 2015, Royal Society of Chemistry.

© 2019 WILEY-VCH Verlag GmbH & Co. KGaA, Weinheim

of Figure 4g, in gravure printing, the ink gets transferred from the inlet on the gravure cylinder.[34] Then, a doctor blade wipes the excess ink from the cylinder. The features are engraved in the cylinder—at this stage, the features are filled with ink. When the cylinder rolls over the substrate the ink is transferred onto the substrate, and the ink spreads to create the final pattern. Multiple gravure cylinders can be connected in series for printing multilayer films as shown in Figure 4h. With gravure printing, it is possible to archive feature sizes of a few µm. For large-area and high-volume manufacturing, gravure is the ultimate choice. Välimäki et al. used a combination of gravure and rotary screen printing for fabricating rolls of inverted organic photovoltaic (OPV) modules, as shown in Figure 4i.[79]

Blade Coating and Slot-Die Coating: Blade coating and slot-die coating both use doctor blades to blanket coat a thin film on the substrate.[29,81] In the case of blade coating, there is no continuous supply of ink, whereas slot-die coaters have a feed line for a controlled continuous supply of ink. The viscosity of the inks used for blade coating and slot-die coating is fairly low (<100 cP), hence, the deposited films are also thin, usually, <1 µm. These processes are compatible with fast high-volume printing techniques. Both electronic and optoelectronic devices can be fabricated using blade coating and slot-die coating. Pierre et al. demonstrated organic transistors and organic photodiodes (OPDs) with blade coating.[29,83] Han et al. reported organic light-emitting diodes (OLEDs) using blade coating.[81]

Spray Coating: Spray coating is a fast and efficient printing method that is used for prototyping as well as in large-scale manufacturing. Using stencils, patterns <100 µm width and with controllable thicknesses (≈1 µm) can be obtained. The feature size is mostly dependent on the features of the stencil. For prototyping, spray coating is cost-effective, and the validated design can be transferred to a rapid printing process such as screen printing. In FHE, passive electronic components, interconnects, and antennas can be manufactured using spray coating. For example, Thielens et al. recently reported a spray-coated antenna that works in the ultrahigh frequency radio-frequency identification (UHF RFID) band.[91]

3D printing has been becoming popular in the last couple of years. Conventional and custom 3D printers are currently being used to fabricate functional electronic circuits. One strategy is to create 3D printed channels, and filling those channels with a liquid metal to get electrical connectivity,[92] and the other strategy is to use conductive metal that is 3D printed.[93] 3D printing is an exciting direction for FHE, however, getting thin and smooth films is challenging with 3D printing. Therefore, the current focus is mostly geared toward printing passive electronics with 3D printers.

Since the choice of printing technique depends on ink properties and printed feature requirements, in **Figure 5**, a comparison of the different printing techniques is provided listing ink and printed feature properties.

2.1.4. Printed Sensors and Circuits

Using different printing techniques, a vast range of sensors and circuits can be fabricated. Printed sensors utilize printed materials to transduce physical quantities such as temperature, light, sound, force, or chemical reaction to electrical signals. For example, in a printed thermistor, the resistance of the printed active material changes with temperature. In recent years, a tremendous amount of work has been done to design printed sensors for wearable health monitoring.[57,58,94] All the vital signs—body temperature, heart rate, respiration rate, blood pressure, and pulse oxygenation can now be measured with printed sensors.[7] In addition to medical applications, printed electrical, optical, and chemical sensors have been demonstrated for energy and environmental applications.[61] Recent developments of printed sensors with applications in health,

Printing properties	Inkjet Printing	Screen Printing	Gravure Printing	Blade Coating	Spray Coating
Ink viscosity	5 – 50 cP	500 – 5000 cP	10 – 1000 cP	<100 cP	10 – 100 cP
Critical linewidth	30 – 70 µm	50 – 150 µm	5 – 100 µm	–	50 – 150 µm
Film thickness	0.1 – 1 µm	5 – 100 µm	0.1 – 1 µm	0.1 – 1 µm	0.5 – 1 µm
Film roughness	Low	High	Low	Low	Medium
Printing speed	0.01 – 0.1 m s^{-1}	0.1 – 1 m s^{-1}	0.1 – 10 m s^{-1}	0.01 – 1 m s^{-1}	0.1 – 1 m s^{-1}
2D patterning	Yes	Yes	Yes	No	Yes
Large-area scalability	Limited	Yes	Yes	Yes	Limited
Design flexibility	High	Low	Low	Medium	Medium

Figure 5. Performance comparison of different printing techniques. Inkjet printing, screen printing, gravure printing, blade coating, and spray coating are compared in term on ink viscosity, critical linewidth, film thickness, film roughness, printing speed, 2D patterning, large-area scalability, and design flexibility.[7,69,78] Adapted with permission.[89] Copyright 2016, University of California.

© 2019 WILEY-VCH Verlag GmbH & Co. KGaA, Weinheim

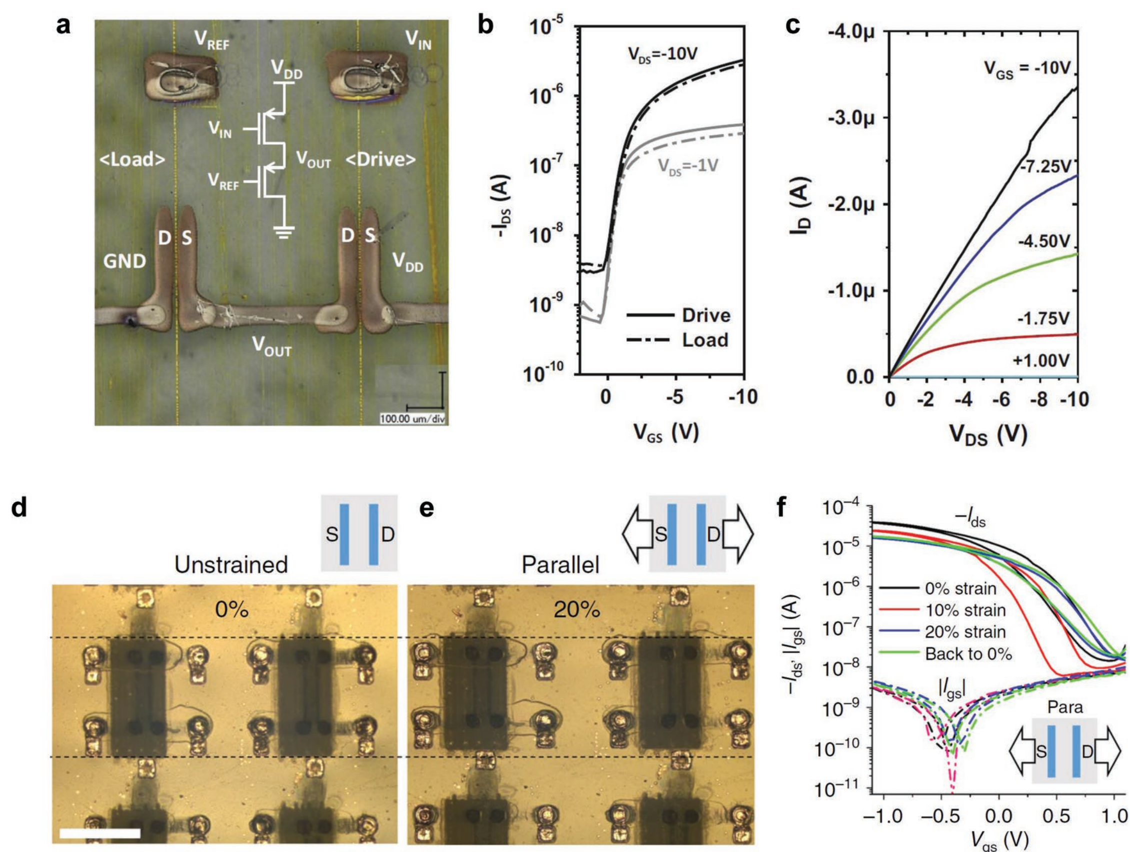

Figure 6. Printed transistors and circuits and their performance parameters. a) Optical microscopy image of an inverter (the circuit diagram of the PMOS inverter is shown in the middle). b) Transfer characteristic of the two transistors in (a). c) Output characteristic of the drive transistor. a–c) Reproduced with permission.[30] Copyright 2014, Elsevier. d,e) Optical microscopy images of stretchable transistors with and without 20% strain. The dashed lines serve to highlight the change in the size of the stretched transistors when compared to the reference transistor (0% strain). The scale bar is 1 mm. f) Transfer and output characteristics of the transistors with and without strain. d–f) Reproduced under the terms of the CC-BY Creative Commons Attribution 4.0 International License (http://creativecommons.org/licenses/by/4.0/).[90] Copyright 2019, The Authors, published by Springer Nature.

structural health, industrial, environmental, and agricultural sensing are provided in Section 3.

Similar to printed sensors, excellent progress has been made in improving printed transistors and circuits. Kang et al. reported printed high-mobility organic thin-film transistors and inverters on plastic substrates that operate in the MHz regime.[30] High-speed gravure printing was used to fabricate sub 5 µm gate electrodes. The printed transistors and their transfer and output characteristics are shown in **Figure 6**a–c. Beside plastic substrates, elastomeric substrates can also be used to fabricate sensors and circuits—making them stretchable. Wang et al. demonstrated an intrinsically stretchable transistor array with a device density of 347 transistors per square centimeter.[95] Molina-Lopez et al. used inkjet printing of polymers and carbon nanotubes to fabricate stretchable transistor arrays with mobilities of 30 $cm^2 V^{-1} s^{-1}$.[90] The fabricated devices with and without strain are shown in Figure 6d,e, respectively. The transfer and output characteristics of the transistors are shown in Figure 6f. Apart from digital and analog electronics, printed circuits can also be used for sensing applications. Zhu et al. reported a temperature sensor based on stretchable carbon nanotube transistors.[48] Despite significant progress, printed circuits are still not on par with silicon ICs in terms of stability and performance. Hence, silicon ICs continue to dominate FHE implementations.

2.2. Thinned Silicon ICs

2.2.1. Thinning Silicon ICs and Connecting to FHE

Silicon ICs are an integral part of FHE. In the past few years, various materials and methods have been utilized to mount silicon ICs and rigid electronic components onto flexible substrates.[53,54] In this section, we discuss the different form factors of silicon ICs and other rigid components, and review possible bonding processes and materials.

The most common rigid components used in FHE systems are silicon ICs. These are needed for communication, data storage, and simple or complex signal processing. Normally, silicon dies are packaged in thermoplastic filled with glass particles, and the connections from the dies are brought out using metal leads. Depending on the complexity of the ICs, packages are 2–10 mm in length and width, and 0.5–2 mm thick, with

© 2019 WILEY-VCH Verlag GmbH & Co. KGaA, Weinheim

4–48 contacts pads (these numbers reflect only the ICs pertinent to FHE). Some packages come with metal leads, while some do not. The leads are typically on the order of a few tens to hundreds of μm wide, and spaced at few tens to hundreds of μm.

Thinned silicon ICs are particularly interesting for FHE as they can be bent or flexed with the flexible substrates. A significant amount of work has been done to create ultrathin silicon ICs that are ≈25 μm thick and can be bent to a radius of curvature of 5 mm.[96] As shown in **Figure 7**a, pre- and post-processing of silicon and silicon on insulator wafers can be used to realize thinned silicon ICs. Selective removal of silicon can be done using grinding, dry or wet etching, chemical reaction, or a combination of them.[99–101] It is also possible to obtain semitransparency in the thinned flexible silicon. Rojas et al. used a combination of a hard mask deposition, trench etching through the hard mask and silicon by deep reactive ion etching, and XeF_2-based isotropic etching to obtain mechanically flexible and semitransparent silicon (Figure 7b).[97] Another variant of thinned silicon are fabricated on a polymer substrate—currently, system-on-chip silicon modules are available that are ultrathin and flexible for FHE usage (Figure 7c,d).[98] In traditional ICs, connection from the die to the package is made using wire bonding. In the case of thinned silicon, to interface with printed sensors and circuits, an interposer is required that fans out the signal to a pitch spacing (>100 μm) that is compatible with printing (Figure 7e).

Apart from silicon ICs, passive components such as resistors, capacitors, and inductors are necessary for FHE. Mostly, surface mounted devices (SMDs) are integrated into FHE to get circuit functionalities. Although it is possible to print flexible passive components, if the required value is high, they tend to have a large footprint.[15] In RF applications, inductors and capacitors are used for impedance matching. Matching networks could be made with printed stub transmission lines, but the matching networks would be about as large as the printed antenna, and the associated resistive losses might hamper performance. In such circumstances, using conventional SMDs could be beneficial. These components come in a variety of sizes and are specified by their dimensions. For example, 0402 components are 0.04 in. by 0.02 in. (1 mm by 0.5 mm). Niittynen et al. studied techniques for attaching SMDs with inkjet-printed traces, comparing materials and volume of conductive adhesives. Conductive adhesives adhere very well to the inkjet-printed traces and SMDs, and failures occur at the SMDs' coating. Isotropic conductive adhesives (ICAs) are not as reliable as solder connections, but with advanced ICA materials and processes, it is possible to reliably connect SMDs to inkjet-printed circuits.[102]

Silicon ICs and passive components are typically connected to flexible substrates with solder or ICA dispensed between the chip and the substrate. A flip-chip pick-and-place tool can be used to align chips. Precise alignment of chip pads to printed traces is required—alignment accuracies of tens of μm are desirable for the bonding tools. Fabrication processes and

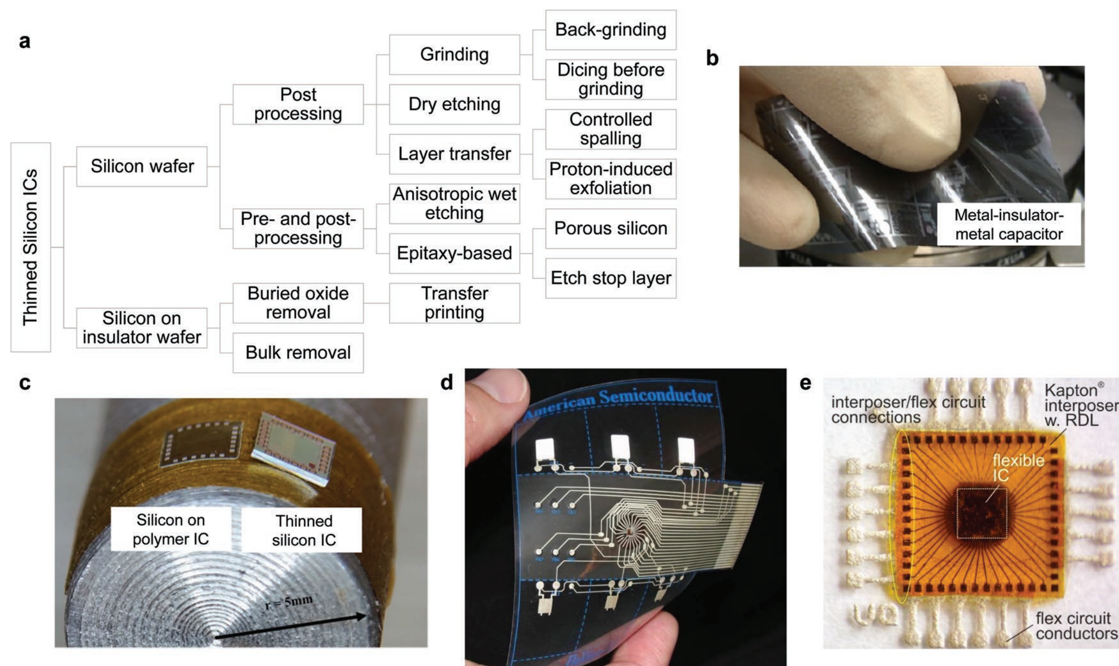

Figure 7. Thinned silicon IC fabrication and assembly with FHE. a) Various techniques that are used to thin down bulk silicon to <25 μm. Selective removal of silicon can be done using grinding, dry or wet etching, chemical reaction, or a combination of them on silicon and silicon on insulator wafers. Adapted under the terms of the CC-BY Creative Commons Attribution 4.0 International License (http://creativecommons.org/licenses/by/4.0/).[96] Copyright 2018, The Authors, published by Springer Nature. b) Semitransparent flexible metal–insulator–metal capacitors manufactured using a combination of a hard mask deposition, trench etching through the hard mask and silicon by deep reactive ion etching, and XeF_2-based isotropic etching. Reproduced with permission.[97] Copyright 2014, ACS Publications. c,d) Flexible silicon on polymer system-on-chip (SoC) mounted on a 5 mm radius-of-curvature mandrell. Photograph of the silicon on polymer SoC integrated into an FHE system. c,d) Reproduced with permission.[98] Copyright 2017, IEEE. e) A flexible thinned silicon IC is interfaced with a plastic substrate using an interposer that fans out the signal to a pitch spacing (>100 μm), which is compatible with printing. Photo provided by and used with permission from Uniqarta, Inc.

© 2019 WILEY-VCH Verlag GmbH & Co. KGaA, Weinheim

materials should be chosen such that the conductive material does not get squished out and short the pads together.

Mounting thinned silicon ICs presents its challenges and opportunities. Thinned silicon ICs are extremely fragile, and conventional assembly equipment can damage the chips. Exposure to heat can warp the chips. They also tend to have very small contact pads. A common solution for interfacing the chips is to embed the ultrathin chip in a film or foil, to create a complete system in foil.[103,104] Ultrathin chips can also be embedded in an interposer film, with fan-out patterns to enable easier integration with printed traces.[17,103] Various transferring techniques can be utilized to transfer silicon ICs to flexible and stretchable substrates.[105–107] The transferred silicon ICs can be flip-chip bonded or pick-and-placed onto flexible and stretchable substrates using a low-temperature solder or adhesive printed electrodes.

2.2.2. Conductive and Nonconductive Adhesives

To attach silicon ICs and passive rigid components solders, conductive adhesives, and printable inks can be used. Sn–Pb solders high reflow temperature (204 °C) restricts its usage for flexible electronics. There are alternative solders that are composed of tin, silver, and bismuth with reflow temperatures <175 °C.[54] Another option is conductive adhesives, which are composed of conductive filler (usually metallic)—small particles or flakes and a polymer binder.[108] Silver is the most commonly used filler because of its high conductivity and low cost. Conductive adhesives are usually cured with heat and pressure to fuse the metal particles into a conductive network.

There are two main classes of conductive adhesives: isotropic and anisotropic. ICAs conduct electricity in all directions, so they are applied in a paste or ink form precisely at the location of each contact. Stencils or screen printing techniques can be used to apply the ink. The size of the openings in the stencil determines the volume of the adhesive, which impacts conductivity and reliability.[102] Anisotropic conductive adhesives (ACAs) conduct only in the z-direction, not in the x–y plane; they have lower filler content than ICAs. ACAs come as pastes or as films. Because they only conduct in one direction, a single piece can be used for all the contacts of a chip without shorting different contacts together.[109] Another alternative for connecting rigid components to FHE is to use conductive ink in either inkjet or screen printable formulations. Similar to conductive adhesives, conductive ink is composed of small conductive particles and a binder dissolved together in a solvent.[110] Conductive ink typically does not have the mechanical strength of a conductive adhesive and so it is sometimes used in conjunction with a nonconductive adhesive. In the case of a tighter pitch (<100 µm), to avoid shorting among the adjacent IC leads, nonconductive adhesive can be printed in between the leads. This electrically isolates the leads, while keeping the IC in place.[111] Also, nonconductive adhesive can be printed on top of the components for final encapsulation. Conductive adhesives can only be applied at conductive interconnects and can thus only provide a limited amount of adhesive force. Additionally, in general, they are not stress-tolerant. Therefore, nonconductive adhesives are commonly added to provide mechanical stability and encapsulation.

2.2.3. Assembly Process for Rigid Components in FHE

In a typical FHE assembly process, printed devices and circuits are fabricated first. Then, the rigid components are assembled. An example process flow is shown in **Figure 8**a, where the substrate is first drilled to create the via holes that connect top circuitry to the bottom circuitry. Then, the top layer of metal is printed and cured. The substrate is flipped for printing the bottom layer of metal and curing. After that, top and bottom encapsulations are printed leaving only the pads where components will be placed. All the rigid components and silicon ICs are then bonded to the substrate. In this case, a dielectric underfill is used to keep the components in place, and ICAs are used to connect the components to the printed circuit. NextFlex's first-generation printed Arduino is shown in Figure 8b, which was fabricated using the described process flow.

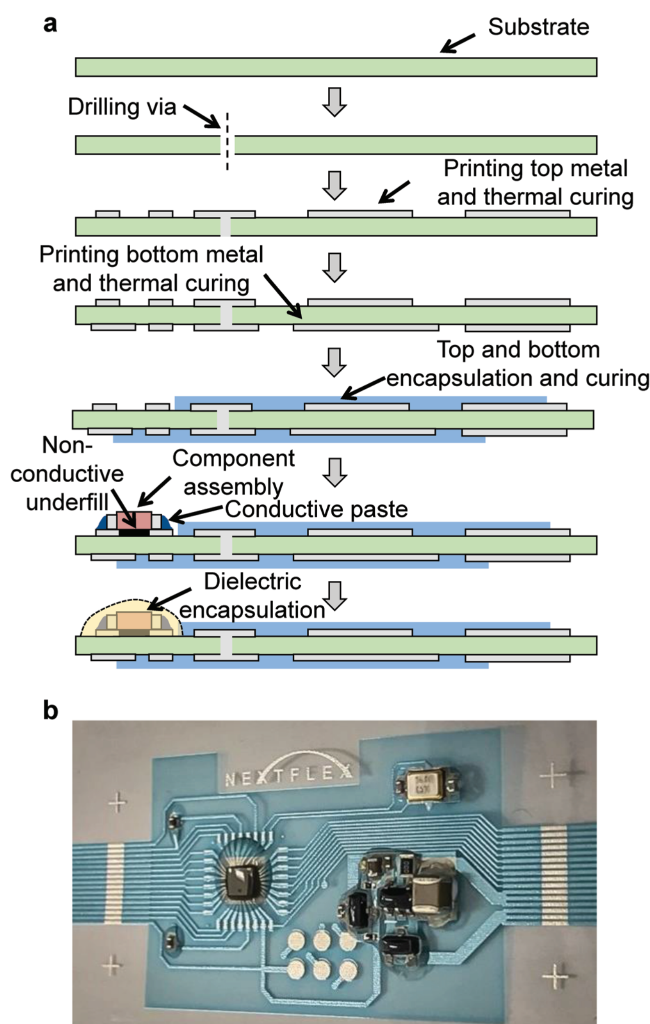

Figure 8. Assembly process and photo of an example FHE system. a) Process steps for printing and assembling FHE systems. b) Photograph of an example FHE system—a printed and flexible Arduino. Photo provided by and used with permission from NextFlex.

© 2019 WILEY-VCH Verlag GmbH & Co. KGaA, Weinheim

2.3. Printed Antennas for Wireless Power and Communications

FHE relies on printed antennas for both wireless communication and power transfer. Wireless communication occurs through electromagnetic fields that are, in the case of FHE, generated by a radio-IC at frequencies (10–6000 MHz), delivered to the antenna, and then communicated over the air. Wireless charging, on the other hand, occurs at lower frequencies (10–50 MHz) and usually through inductive coupling using a loop antenna. There are wireless technologies such as near-field communication (NFC) or RFID that allow for both communication and charging using the same antenna and system. While we focus on printed flexible antennas in this paper, it is worth noting that there are alternative techniques to fabricate flexible antennas. Flexible antennas have been demonstrated using etching[112,158,159] or cutting[160] of thin conductors or conductive tapes on a flexible substrate, using conductive textiles,[140] liquid conductors[161] embedded in a flexible casing, drop-casting on flexible substrates,[113] and sputtering of copper on a flexible substrate.[162]

2.3.1. Printed Antennas for Communication Purposes

Table 2 lists an overview of the literature on printed, flexible antennas for wireless communications. There are several printing techniques proposed in the literature to print antennas or print wireless FHEs. Reviews of printing techniques for antennas can be found in refs. [114,115]. Inkjet printing and screen printing are the most commonly used techniques. However, spray-coated, stencil-printed, gravure-printed, and direct-write printed antennas have also been demonstrated. Wireless FHEs are almost solely fabricated using inkjet or screen printing. These techniques provide high resolution, which is necessary for the chip-mounting on printed traces, see Section 2.2. The used ink type is predominantly silver nanoparticle ink, regardless of the printing technique, antenna type, or used communication frequency. Some carbon-based inks are used for flexible antenna printing as well. Conductive traces made by silver nanoparticle inks can, after curing, deliver conductivities $>10^6$ S m^{-1}, which is necessary to reduce resistive losses in the antennas. High conductivity is necessary to increase antenna efficiency and (effective) gain. The most studied wireless technologies, see Table 2, are UHF RFID around 0.9 GHz and wireless local area networks (WLAN) and Bluetooth, that both operate in the license-free industrial scientific and medical (ISM) frequency bands around 2.45 and 5 GHz. Note that most commercially available radio ICs also operate in these frequency bands. The bulk of the studies in the literature focus on dipole and monopole antennas. These antennas are relatively simple, with planar antenna configurations. The simplicity is largely because it is difficult to create cavities, vias, or multilayer structures on flexible substrates, which are necessary to create more complex antennas.

Table 2. Literature overview of printed and flexible antennas.

Printing technique	Antenna type	Target frequency band	Surface area [mm × mm]	Antenna gain [dBi]	Ref.
Inkjet printing	Dipole	UHF RFID[a]	95 × 50 to 122 × 50	1.5 up to 2.1	[110,112–117]
		ISM 2.4[b]	60 × 32	–10.5	[118]
	Monopole	UHF RFID	70 × 70 to 80 × 136	–1.2 to 2.6	[110,119]
		ISM 2.4	25 × 27 to 127 × 87	0.2–4.8	[119–123]
		ISM 5[c]	40 × 35 to 59 × 31	2.36–4	[121,123,124]
	Slot	UHF RFID	–	–13 (on ground plane)	[125]
		ISM 2.4	59 × 31	1	[126]
	Patch array	ISM 5	114 × 52	10	[127–129]
Screen printing	Dipole	UHF RFID	82 × 19 to 136 × 28	–4 to 1.6	[130–135]
		ISM 2.4	>11 × 59	2.2	[136]
		1.8–4 GHz	–	–	[137]
	Slot	Wimax	44 × 161	7	[138]
Stencil printing	Slot	UHF RFID	65 × 20	–16	[139]
	Monopole (array)	3 GHz and 6 GHz	45 × 48 (single antenna)	0.37 (single 3 GHz) 4.9 (array at 6 GHz)	[140]
	Dipole	ISM 2.4	–	–	[141]
Spray coating	Dipole	UHF RFID	52 × 44 to 48 × 46	0.8–7.4 (on ground plane)	[137,142]
	Slot	UHF RFID	56 × 111	2	[143]
Direct-write printing	Inverted F	ISM 2.4	46 × 30	1.2	[144]
	Dipole	ISM 2.4	–	–	[143]
Gravure printing	Dipole	UHF RFID	–	–	[118,144,145]

[a]UHF RFID (902–928 MHz); [b]ISM 2.4: Industrial, scientific and medical, license free band around 2.45 GHz. Including applications such as WLAN, WiFi, Bluetooth, etc; [c]ISM 5: Industrial, scientific and medical, license free band around 5 GHz. Mainly used for WiFi.

© 2019 WILEY-VCH Verlag GmbH & Co. KGaA, Weinheim

One of the most important antenna parameters is an antenna's gain. This quantity is the product of the directivity (how well an antenna can deliver power in a certain direction in comparison to an isotropic antenna) and the antenna's efficiency (radiation times mismatch efficiency), and is usually expressed in dBi, a logarithmic ratio of the antenna's gain relative to the one of an isotropic antenna. The antennas listed in Table 2 are designed and characterized to have a good (>90%) mismatch efficiency in the frequency bands listed in Table 2. However, radiation efficiency and directivity depend strongly on the antennas' design, material parameters, frequency of operation, and surface area. The gains of the flexible, printed antennas listed in Table 2 range from −16 to 10 dBi. In general, an antenna that uses a larger volume (in the case of printed antennas on thin flexible substrates, this mainly comes down to the occupied surface) has the potential to have a higher antenna gain. **Figure 9** shows a scatterplot of the antenna gains presented in those references listed in Table 2 versus the antenna diameter over the wavelength. Higher gains are highly correlated with higher relative diameters $r_{corr} = 0.82$ (Pearson, $p < 0.01$) and $r_{corr} = 0.56$ (Spearman, $p < 0.01$). This illustrates the main trade-off facing antenna design for FHE—a small footprint is desirable, but this leads to a lower gain and consequently a lower range, higher power consumption, and worse signal quality.

2.3.2. Printed Coils for Wireless Power Transfer

An alternative and more efficient than RFID technology for wireless energy transfer is inductive wireless power transfer (WPT), which has been standardized by the wireless power consortium (WPC). WPT usually operates between 12 and 16 MHz.[163] **Table 3** lists an overview of printed, flexible coils used for inductive WPT. Nearly all the coils that can be found in the literature are printed using silver-based inks. Gravure, inkjet, and screen printing are used to fabricate these coils. Earlier studies investigated optimized solutions of silver inks for gravure and inkjet printing of multiturn coils for RFID or WPT purposes[149,152–155,157] and optimized the number of turns, with generally more turns leading to smaller antennas, but not necessarily better performance. In a further step of development, these parameters were used to build passive, wireless sensors, where the coil designs[149,152–154,157] were used for sensing of oxygen,[148] gas,[63] electrochemical potential,[150,151] temperature,[136,156] and humidity.[136]

It is also worth noting that besides WPT, NFC, and RFID-based solutions, there are experimental studies that try to design antennas for wireless power harvesting in other frequency bands. Adami et al. demonstrated a screen-printed patch antenna on a flexible polycotton substrate for WPT at 2.45 GHz,[164] while Yang et al. investigated the use of

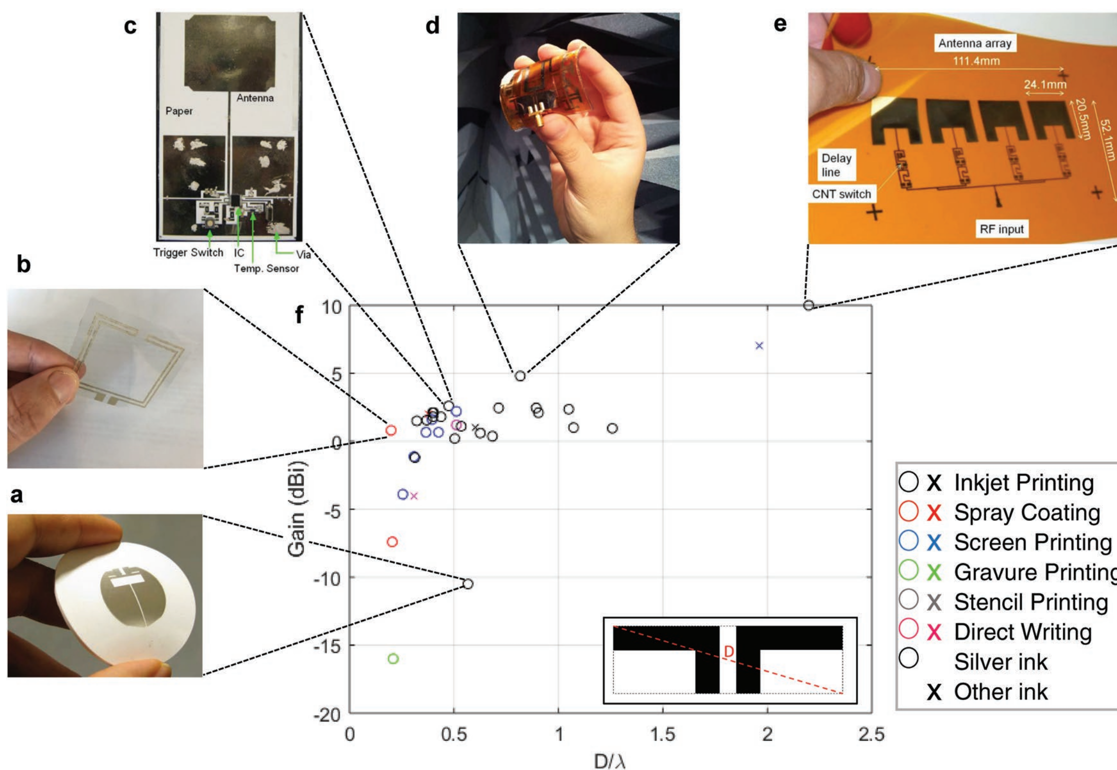

Figure 9. Overview of flexible and printed antenna gains versus antenna dimensions with some notable examples. a) UHF RFID slot antenna on PDMS/ceramic substrate on a ground plane. Reproduced with permission.[127] Copyright 2012, IEEE. b) Spray-coated folded dipole antenna on PEN. Reproduced with permission.[91] Copyright 2018, IEEE. c) FHE system on paper with monopole antenna. Reproduced with permission.[146] Copyright 2009, IEEE. d) Inkjet-printed antenna on electromagnetic bandgap surface. Reproduced with permission.[126] Copyright 2013, IEEE. e) Inkjet-printed patch antenna array. Reproduced with permission.[147] Copyright 2012, IEEE. f) Scatterplot of antenna gain versus relative antenna diagonal (*D* over wavelength (λ)) for flexible, printed antennas (sources in Table 2). Colors show different printing techniques, while different marker styles indicate different ink types.

© 2019 WILEY-VCH Verlag GmbH & Co. KGaA, Weinheim

Table 3. Overview of printed coils on flexible substrates for wireless power transfer.

Printing technique	Number of turns in the coil	Substrate	Ink type	Surface area [mm × mm]	IC used	Application	Ref.
Screen	7	PEN	Silver	65 × 40	SL13A (AMS)	Gas sensing—oxygen	[63,148]
Gravure	4–8	PET	Silver	95 × 55	Printed circuit	Electrochemical	[149–151]
Gravure and inkjet	5–6	PET	Silver	80 × 50	None	None	[152]
Inkjet	5	Kapton	Silver	74 × 47	None	None	[153]
Inkjet	10	Kapton	Silver	45 × 45	None	None	[154]
Inkjet	4	Kapton	Silver	86 × 54	None	None	[155]
Inkjet	4	Paper/Flex ferrite	Silver	75 × 45	–	Temperature	[156]
Gravure	1–6	PET	Silver	–	Printed circuit	None	[157]
Screen	6	Kapton	Silver	75 × 45	M24LR64 (ST)	Temperature and humidity sensing	[136]

screen-printed dipole antennas on flexible cellulose membranes at even higher frequencies (8–12 GHz).[165]

2.4. Printed Power Sources—Batteries, Solar Cells, and Energy Harvesters

One of the greatest challenges in developing FHE is providing adequate electrical power for the various system components. Not only do the sensors themselves require power, but also power must be supplied to the electronics that collect, process, and display the data from the sensors. Many modern electronics are designed around the form factor of commercially available batteries (e.g., cylindrical and coin) which are rigid, bulky, and have large footprints.[166,167] In FHE systems, power sources are designed to supply the power needed without limiting mechanical flexibility. For independently operating FHE, on-board energy harvesting and storage is an excellent alternative to rechargeable options that require ports or plugging in cables, for charging. To increase the capacity of these power sources, the area of energy harvester or volume of material must also scale up accordingly. With many systems involving power sources that are directly integrated on the same substrate as the electronics they power,[168–170] it is important to determine the proper chemistry to match the power requirements of the system. This section will discuss the various power requirements specific to FHE systems, as well as the technologies available to provide the required power.

2.4.1. Printed Energy-Storage Modules

For FHE that is designed to be disposable, or has a replaceable energy storage system, a primary, nonrechargeable battery is a good option. These types of batteries are widely used in commercially available portable devices today. As mentioned, because most of the standard primary battery form factors are noncompliant, such as coin cells or cylinders, flexible and stretchable primary batteries have been developed for use in a variety of flexible electronics.[171–174]

As for rechargeable batteries, lithium-ion is the predominant chemistry, due to its particularly high energy density, power density, and long lifetime.[175] Most lithium-ion batteries follow a sandwich architecture due to the low conductivity of the solid electrolytes used to fabricate them. There have been reports of lithium-ion batteries in the parallel configuration, and this geometry comes with increased mechanical compliance. Also, flexible (**Figure 10**a),[170] stretchable (Figure 10b),[176] cable (Figure 10c),[177] even tattoo (Figure 10d,e)[169] form factors have been demonstrated using rechargeable lithium-ion chemistry. Singh et al. demonstrated a lithium-ion battery where all the components of the battery were deposited using primarily spray coating. The cells had a nominal voltage of 2.5 V and a capacity of 30 mAh with an active area of 25 cm^2. This was integrated with a polycrystalline solar cell for charging and 40 light-emitting diodes (LEDs) for discharging.[178]

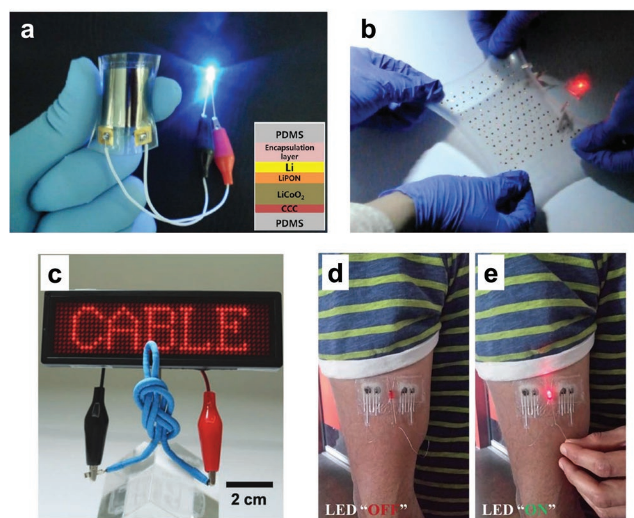

Figure 10. Batteries with different form factors for flexible hybrid electronics. a) A flexible lithium-ion battery turning on a blue LED under bending. The inset shows the material stack used in the battery. Reproduced with permission.[170] Copyright 2012, ACS Publications. b) A stretchable lithium-ion battery with self-similar serpentine geometries powering a LED under a biaxial stretch of 300%. Reproduced with permission.[176] Copyright 2013, Springer Nature. c) A cable battery of length 25 cm used to power a red LED screen. The cable battery exhibited stable operation even when twisted. Reproduced with permission.[177] Copyright 2012, Wiley-VCH. d,e) A temporary tattoo battery lighting an LED. Reproduced with permission[169] Copyright 2014, The Royal Society of Chemistry.

© 2019 WILEY-VCH Verlag GmbH & Co. KGaA, Weinheim

Other alkaline chemistries, such as silver–zinc and zinc–manganese are less toxic and less reactive than rechargeable chemistries; they can be processed in air and have fewer restrictions on encapsulation. One of the first intrinsically stretchable batteries was demonstrated by Kaltenbrunner et al., where they used zinc/manganese dioxide (Zn/MnO_2) as the active material in the battery. Carbon black was printed onto an elastomer, and Zn and MnO_2 were printed on top of the current collectors to form the anode and cathodes respectively. An electrolyte gel was then printed in between the layers and the battery was encapsulated by laminating the whole stack with another acrylic elastomer. The battery was able to continuously power a green LED even after stretching to 100% strain.[181]

Besides the common flat and flexible form factor for compliant batteries, other geometries are interesting to consider for FHE applications. Wire batteries have been demonstrated in the literature, with interesting mechanical properties. Due to the nature of having a metal wire serve as the current collector, the hollow structure of these batteries absorbs the externally generated stresses efficiently, by physically deforming the battery.[180] Kwon et al. demonstrated a cable-type lithium-ion battery, where the battery consisted of several electrode strands coiled into a hollow spiral for the anode, with a PET separator and cathode slurry on the outside.[177] This cable battery was robust and can be woven into many different shapes and forms, and even used as an interconnect itself to connect different components of an FHE system. It is worth mentioning that these nonflat batteries are not fabricated using printing techniques. However, the materials are compatible with printing technologies, hence, can be adapted for use in FHE.

2.4.2. Printed Energy-Harvesting Modules

Solar power is the most abundant energy source in nature and is often harvested, to power a variety of electronics. However, the amount of light available for capture varies several orders of magnitude from being outdoors in a clear sunny day, to indoors in a dimly-lit room. Depending on how the solar cells are optimized, the available power density from photovoltaics (PV) can vary from 100 mW cm^{-2} in sunlight to less than 500 μW cm^{-2} indoors. Unfortunately, because of this high variation in power density, it would be difficult to reliably power electronics purely based on solar energy. Instead, using PV in conjunction with an energy storage device, such as a battery, could compensate for the variation in light intensity and ultimately provide a reliable system for powering FHE.

OPVs primarily use semiconductor polymers or small molecules as the active layer. OPVs can be fabricated with a very thin total thickness, with some reports of modules less than 3 μm.[185] This is very appealing for FHEs, especially because the substrates used for the OPVs are compatible with many other processes used to fabricated devices, sensors, and energy storage. OPVs have been demonstrated with maximum efficiencies of 10–11%, similar to amorphous silicon cells, and can potentially reach higher efficiencies under indoor lighting. In particular, solar cells that have been optimized by Lechêne et al. have shown a maximum of 7.6% power conversion efficiency (PCE).[84]

Integrating solar cells with batteries provide an elegant solution for powering FHE because the whole system becomes self-powered. Ostfeld et al. combined silicon solar cells with printed batteries to create a flexible power source that is wearable (**Figure 11**a,b), and can be integrated with smart objects (Figure 11c,d).[179] Another example of an integrated PV and energy storage system was demonstrated by Zamarayeva et al., where a stretchable wire-shaped battery was combined with a solution-processed OPV, in the form of a wearable bracelet (Figure 11e,f). When the solar charging rate was matched with the electrical load (a sensor), the bracelet did not require additional charging to power the sensor (Figure 11g).[180] These self-powered systems are great for FHE, as they can be designed with years of lifetime without needing to replace the power source.

2.5. Printed Display Modules

Two different strategies are usually employed to retrieve sensor data from FHE—1) FHE wirelessly transmits the data to a remote host, and 2) the data are shown on a display that is part of the FHE. As an example of the first strategy, in a wearable sensor patch, Khan et al. used a wireless communication module and an external display device—a mobile phone, to present sensor data to the user.[53] In the second strategy, the system takes a fully integrated approach, with the display directly fabricated on the same substrate as an FHE component.[45] Depending on how the data is being visualized, different displays may be required. Certain information can be communicated to the user simply with a series of indicator lights, whereas some applications require a seven-segment display. There are multiple ways of realizing flexible displays, including processes that involve photolithography, however this section will primarily review developments on solution processable, flexible displays that are or can be integrated into FHE.

Electrochromic displays are low-power, low-cost, and printable, which makes them a great candidate for use in FHE. Due to the paper-like thin form factor, electrochromic displays coined the term e-paper.[186] **Figure 12**a shows an example of an electrochromic display connected to a printed temperature sensor that lets the user know when the temperature exceeds a certain limit.[45] To demonstrate the integration of electrochromic displays with printed transistors, Cao et al. reported a fully screen-printed active-matrix electrochromic displays employing carbon nanotube thin-film transistors in the backplane (Figure 12b).[182] OLEDs are also getting popular as a display candidate for FHE—both vacuum- and solution-processed OLEDs can be used with printed sensors. Yokota et al. demonstrated an extremely thin seven-segment display fabricated with chemical vapor deposition (Figure 12c).[183] Han et al. used a combination of screen printing and blade coating to print a seven-segment display (Figure 12d).[82] Furthermore, a stretchable quantum dot LED (QLED) display has been demonstrated (Figure 12e),[184] which is promising for displaying sensor data. Overall, an encouraging amount of progress has been made in the printed display technologies that can be adapted for FHE.

© 2019 WILEY-VCH Verlag GmbH & Co. KGaA, Weinheim

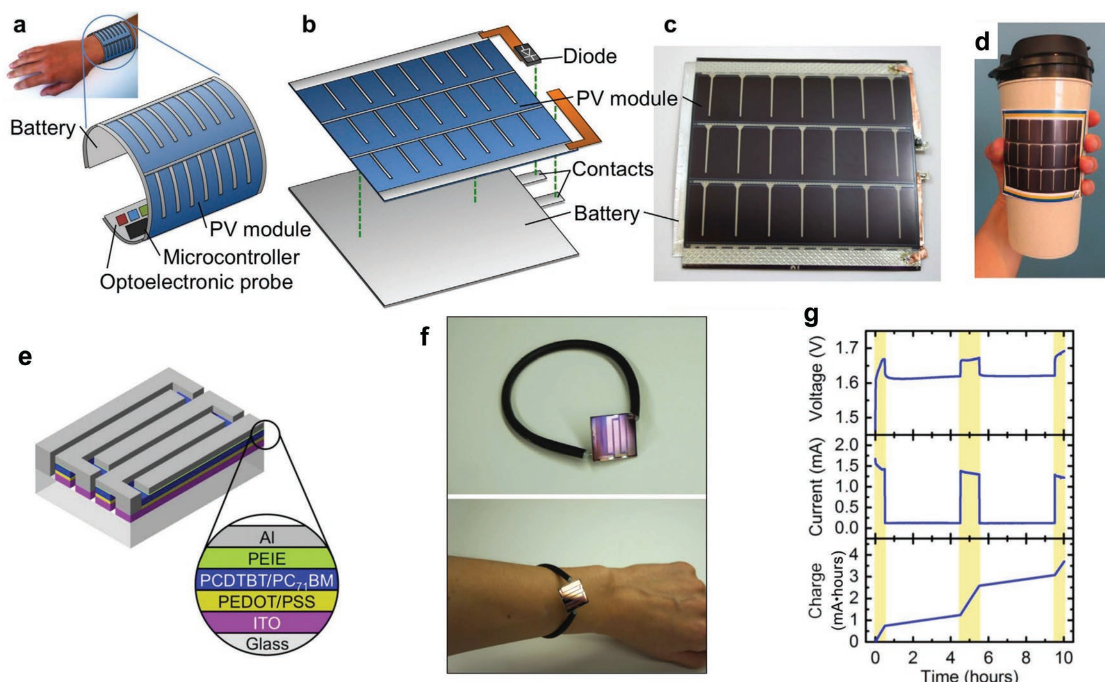

Figure 11. Flexible and stretchable self-powered systems for FHE. a–d) A silicon solar cell is combined with a lithium-ion battery to create a flexible self-powered source that is wearable. Due to the flexibility, the integrated power source and storage module can be used to power smart objects—in this case, a travel mug. a–d) Reproduced under the terms of the CC-BY Creative Commons Attribution 4.0 International License (http://creativecommons.org/licenses/by/4.0/).[179] Copyright 2016, Springer Nature. e,f) Integrated flexible wire battery combined with a solution-processed OPV. e) OPV device structure. f) Silver–zinc wire battery connected to the OPV in a wearable bracelet form factor. g) Voltage, current, and cumulative stored charge of solar battery charging during a simulated day of use. The yellow shaded areas indicate periods of exposure to sunlight. The white areas correspond to compact fluorescent lamp (CFL) lighting with an illuminance of 3000 lx. Once the discharge rate by the sensor is matched with the charging rate by the OPV, the whole system does not require additional charging. e–g) Reproduced with permission.[180] Copyright 2017, The Authors, published by American Association for the Advancement of Science (AAAS). Reprinted/adapted from ref. [180]. Copyright 2017, The Authors, some rights reserved; exclusive licensee American Association for the Advancement of Science. Distributed under a Creative Commons Attribution NonCommercial License 4.0 (CC BY-NC) http://creativecommons.org/licenses/by-nc/4.0/.

3. Applications of FHE

3.1. Wearable Health Monitoring with FHE

Healthcare is the biggest application area of FHE. Flexible, stretchable, and conformable electronics can mold to the curves of the body in ways rigid electronics cannot. Researchers are designing comfortable skin-like electronics devices that monitor vital signs,[7] healing stages of skin wounds,[194,195] and monitor analytes in bodily fluids.[196,197] Most of the biosignals such as temperature, heart rate, respiration rate, blood pressure, pulse oxygenation can now be measured with wearable electronics that utilize FHE architecture. These smart sensors enable in-home health monitoring cutting expensive and long hospital stays.

There are many commercially available wearable devices which provide feedback on the wearer's fitness and encourage a healthy lifestyle. In the academic domain, a vast number of sensors are demonstrated in a band-aid and peel-and-stick form factors.[187] The span for a medical device is not restricted only to sensing devices—controlled drug release devices can now be used for managing diseases.[193]

Common biosignals such as electrocardiogram (ECG) and photoplethysmogram (PPG) provide ample information on the cardiac and physiological health of a person. For example, heart rate, blood pressure, and blood oxygenation information can be collected from two-wavelength PPG. Since these biosignals can be measured noninvasively with wearable devices, in recent years FHE systems are being extensively used to measure ECG and PPG. ECG requires two electrodes to measure a voltage that originates at the heart. PPG, on the other hand, is an optical measurement that uses light attenuation through blood and tissue to calculate heart rate, blood pressure, and blood oxygenation. Demonstrating a wearable ECG FHE system, Khan et al. used two printed gold electrodes and a printed thermistor to measure ECG signals and body temperatures of volunteers (**Figure 13**a,b).[53] The collected ECG signal was pristine as shown in Figure 13c. In a similar demonstration, Jeong et al. used a tattoo form factor electrode pair to measure ECG. The system used an NFC protocol to transmit sensor data (Figure 13d,e).[187] Here also, the collected ECG signal was pristine (Figure 13f). Chung et al. combined both ECG and PPG sensor in a binodal sensor, and applied the system on neonates (Figure 13g,h).[188] The binodal sensor system performed on par with commercial sensors while being skin-like and soft (Figure 13i).

Another wearable health sensing modality is biochemical. Biochemical sensors measure analytes, enzymes, hormones, etc. in bodily fluids. Typically, these sensors use an ion-sensitive membrane on top of an electrode and monitor the potential change

 © 2019 WILEY-VCH Verlag GmbH & Co. KGaA, Weinheim

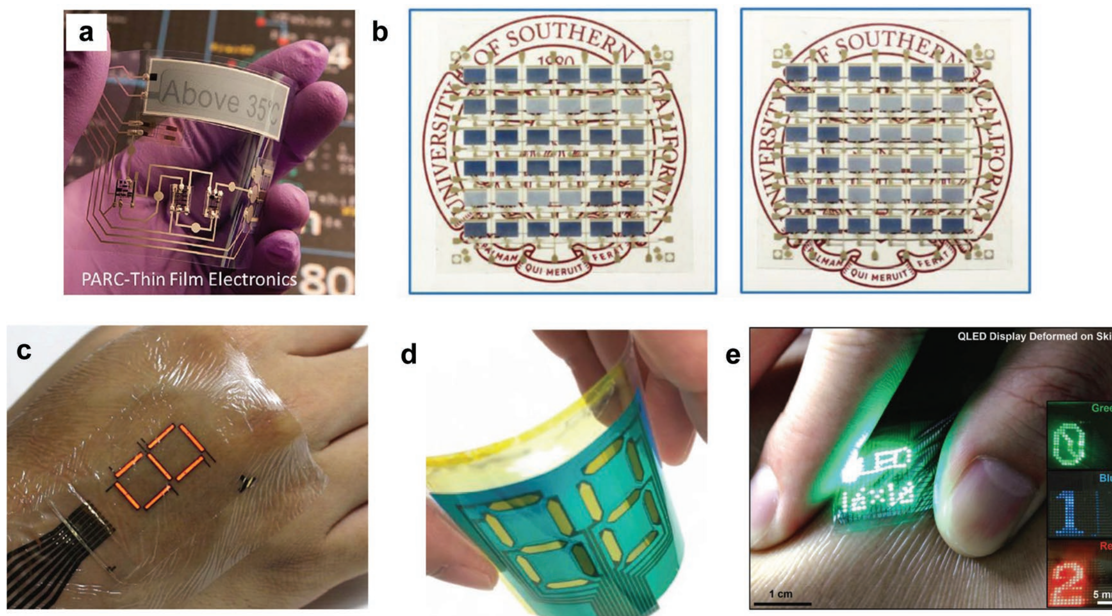

Figure 12. Flexible displays for FHE. a) An electrochromic display (Acreo) showing sensor data from a temperature threshold sensor tag. Reproduced with permission.[45] Copyright 2015, IEEE. b) A 6 × 6 active-matrix electrochromic display, produced by screen printing. Reproduced with permission.[182] Copyright 2016, American Chemical Society. c) Analog OLED seven-segment display produced using chemical vapor deposition (CVD). Reproduced with permission.[183] Copyright 2016, The Authors, published by AAAS. Reprinted/adapted from ref. [183]. Copyright 2016, The Authors, some rights reserved; exclusive licensee American Association for the Advancement of Science. Distributed under a Creative Commons Attribution NonCommercial License 4.0 (CC BY-NC) http://creativecommons.org/licenses/by-nc/4.0/. d) A solution-processed flexible seven-segment display printed using doctor blade coating and emission area patterning technique. Reproduced with permission.[82] Copyright 2018, Wiley-VCH. e) 16 × 16 stretchable quantum dot LED (QLED) stretchable display, produced by thermal evaporation and spin coating. Reproduced with permission.[184] Copyright 2017, Wiley-VCH.

with respect to a reference electrode. Gao et al. integrated multiple sensors in one sensor platform and performed potentiometric and amperometric measurements (**Figure 14**a). The sensor was part of a wrist band, hence, it was able to measure potassium, sodium, glucose, and lactate concentration in the sweat of volunteers while working out (Figure 14b,c).[189] A similar platform with one sensor was demonstrated by Rose et al., where the sweat sensor in a band-air form factor was used to monitor sodium ion concentration (Figure 14d–f).[190] Kim et al. developed a mouthguard that can monitor salivary uric acid levels. Here, the sensor was interfaced with silicon ICs and a Bluetooth transceiver for data processing and communication (Figure 14g–i).[191]

Apart from vital signs and biochemical monitoring, FHE can be used for diagnostics and therapeutics. Wound monitoring and drug delivery systems can leverage soft sensors. Swisher et al. demonstrated a smart bandage that uses printed gold electrodes to perform impedance spectroscopy on the tissue for early-detection of pressure ulcers.[194,195] Khan et al. used arrays of OLEDs and OPDs to measure blood and tissue oxygenation. The reflectance-mode sensor measured oxygenation on various parts of the body, which is not possible with commercial transmission-mode oximeters (**Figure 15**a,b). The sensor was used to accurately measure the oxygenation of volunteers under normal and ischemic conditions (Figure 15c).[192] For therapeutics, FHE can be designed to release drugs in a closed-loop manner. For example, Mostafalu et al. used an FHE smart bandage that delivered antibiotics when the pH of the skin went below a threshold (Figure 15d–f).[193]

In recent years, exciting progress has been made in FHE-based wearable medical devices. With the development of flexible, stretchable, transparent, breathable, biocompatible, and lightweight sensors, we can expect steady progress of FHE in the biomedical space.

3.2. Industrial, Environmental, and Agricultural Monitoring with FHE

In the last few years, the application of flexible and stretchable sensors for industrial, environmental, and agricultural monitoring has taken off. Low-cost and large-area scalability of printed sensors make them an ideal candidate for use in the mentioned application areas. Many of these sensors have wireless functionality, which gives them an advantage over wired sensors. As discussed in Section 2.3, most of such printed, wireless systems operate in an RFID frequency band. Printed RFID labels have been developed to be placed on products for logistics/tracking fragile, delicate, perishable, or expensive goods. Usually, such tags contain a silicon IC, a printed antenna, and printed sensors. **Table 4** provides an overview of systems demonstrated in the literature that measure different environmental signals.

Printed temperature sensors either use a printed thermistor to perform resistive measurements or rely on temperature measurements[62,198,199] of a built-in temperature sensor in the surface-mounted radio frequency IC (RFIC).[134] Most of such printed temperature sensors show a dependency on humidity as well. Therefore, both temperature sensors and humidity sensors are usually calibrated for both quantities.[62] Printed humidity sensors are demonstrated using a variety of measurement

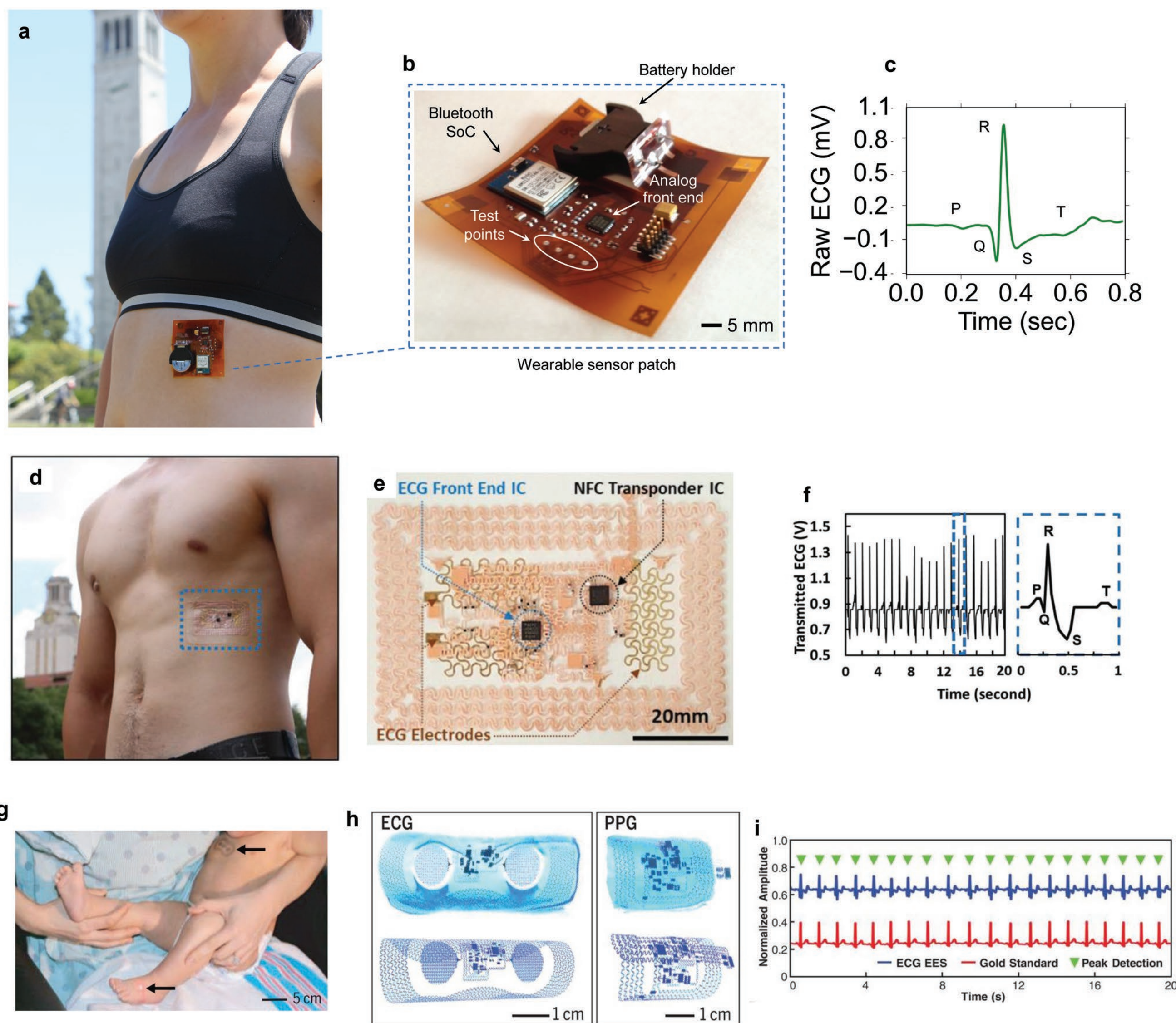

Figure 13. Wearable FHE sensor systems for monitoring vital signs. a,b) A wearable sensor patch composed of an ECG electrode pair and a printed thermistor mounted on the lower left ribcage of a volunteer. The sensors are connected to silicon ICs that processes the sensor data and wirelessly transmits to a remote host via Bluetooth. c) A zoomed-in view of the collected ECG signal. a–c) Reproduced with permission.[53] Copyright 2016, Wiley-VCH. d,e) A peel-and-stick form factor wearable ECG patch. The patch uses an analog front end to process the sensor data, and NFC protocol to transmit the data to a remote host. f) A zoomed-in view of the collected ECG signal. d–f) Reproduced with permission.[187] Copyright 2019, Wiley-VCH. g,h) Wearable ECG and PPG sensors for neonates. The arrows show sensor placement locations. The binodal sensor collects ECG and PPG data, then processes and transmits data to a remote host using an NFC interface. i) Collected ECG signal compared with commercial electrodes. g–i) Adapted with permission.[188] Copyright 2019, AAAS.

mechanisms performed by external sensors, printed sensors, or a printed antenna—1) by monitoring changes in capacitance of a printed interdigitated electrode (a typical example is shown in **Figure 16**a),[62,198,199,204–206] 2) by measuring changes in resistance of printed conductive traces,[150,200,202,203] and 3) by monitoring shifts in antenna resonance and/or antenna efficiencies.[112,202,207] Humidity sensors are demonstrated both as binary sensors and sensors that can estimate relative humidity (RH) with good accuracy up to 1% RH.[200] Figure 16b shows an example of an RFID antenna that is sensitive to changes in humidity.[207]

Aside from water vapor, other gases can be sensed using printed sensors. Most printed gas-sensors aim at detecting a single gas using a printed sensor. A typical gas sensor is often a printed resistor or capacitor where either the printed traces are sensitive to the chemical or are overlaid by a membrane or layer that is sensitive to the gas that needs to be detected. Ammonia-sensing is shown in the 0–100 ppm range,[62,209] and as a binary sensor in ref. [208]. A printed nitrogen dioxide sensor is demonstrated by Dua et al.,[210] where it is also demonstrated that printed gas sensors are usually sensitive to other chemicals and humidity. An oxygen sensor is shown by Martínez-Olmos et al.

© 2019 WILEY-VCH Verlag GmbH & Co. KGaA, Weinheim

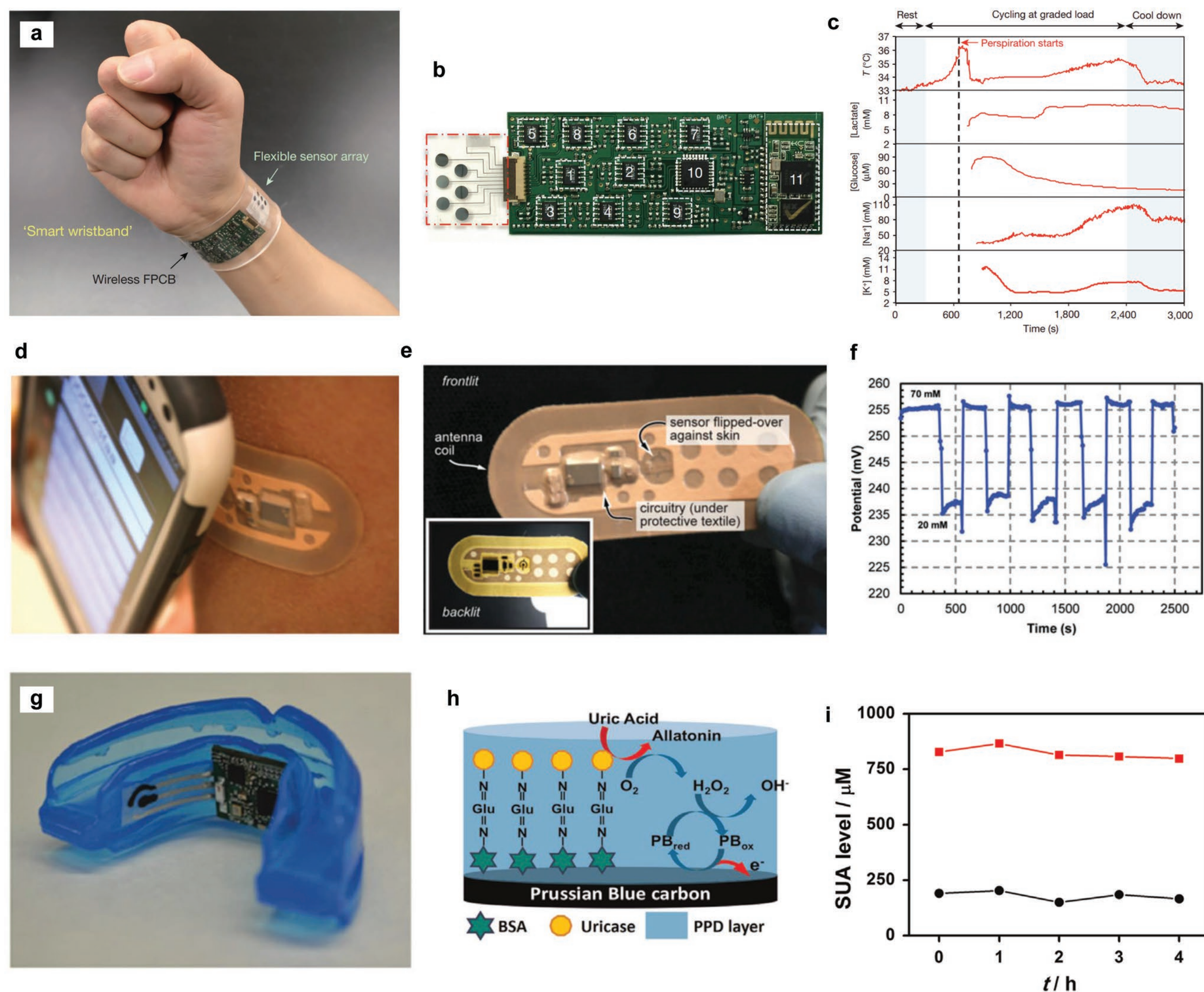

Figure 14. Wearable FHE systems for biochemical sensing. a) A smart wristband composed of multiple biochemical sensors to analyze potassium, sodium, glucose, and lactate concentration in sweat. b) The sweat sensor is connected to an FPCB that hosts silicon ICs to process and transmit the sensor data over Bluetooth. c) A snapshot of the data collected by the sensor system while a volunteer was working out. a–c) Reproduced with permission.[189] Copyright 2016, Springer Nature. d) A band–air form-factor sweat sensor that can monitor the concentration of sodium ions. e) Photograph showing the assembly of the device: the sensor is interfaced with an RFID chip and antenna for wireless transmission of the sensor data. f) Patch data for sodium chloride concentration variation between 70×10^{-3} and 20×10^{-3} M. d–f) Reproduced with permission.[190] Copyright 2014, IEEE. g) An instrumented mouthguard capable of noninvasively monitoring salivary uric acid levels. h) The reagent layer of the chemically modified printed Prussian blue carbon working electrode containing uricase for the salivary uric acid biosensor. i) Monitoring of salivary uric acid level of healthy volunteer (black dots) and a hyperuricemia patient (red squares) obtained with the mouthguard biosensor over a 5 h period. g–i) Reproduced with permission.[191] Copyright 2015, Elsevier.

with surface mounted LEDs and photodetectors mounted on printed silver traces.[148] Finally, multigas sensors (ammonia, oxygen, carbon monoxide, nitrogen dioxide, and humidity) have been developed.[112,201,211] Figure 16c shows an example of a printed, wireless, and flexible multigas sensor using surface-mounted optical reflectometry.[201]

Printed sensors for liquid chemicals have been shown for toluene[212] in the 0–1000 ppm range with 6 ppm sensitivity and ethanol[213] in the 0–320 ppm range. Jung et al. demonstrate a printed circuit that can detect redox reactions and transmits the current–voltage curves associated with such reactions wirelessly.[151] Printed, flexible sensors are also optimally suited for the detection of mechanical forces that might be exerted on packages or stored goods. Strain, pressure, and deformation sensors have been demonstrated in the literature.[137,214,215] Some industrial applications and products are light sensitive. Therefore, printed optical sensors have been shown by Escobedo et al. from ultraviolet to the infrared range.[134]

Most of the printed sensors are sensitive to multiple physical or chemical agents. Therefore, a calibration using multiple exposures is usually recommended.[210] However, some printed sensor nodes use this sensitivity to multiple agents to demonstrate multisensing capabilities.[62,137,201] An example of such a fully printed multisensor platform is shown in

© 2019 WILEY-VCH Verlag GmbH & Co. KGaA, Weinheim

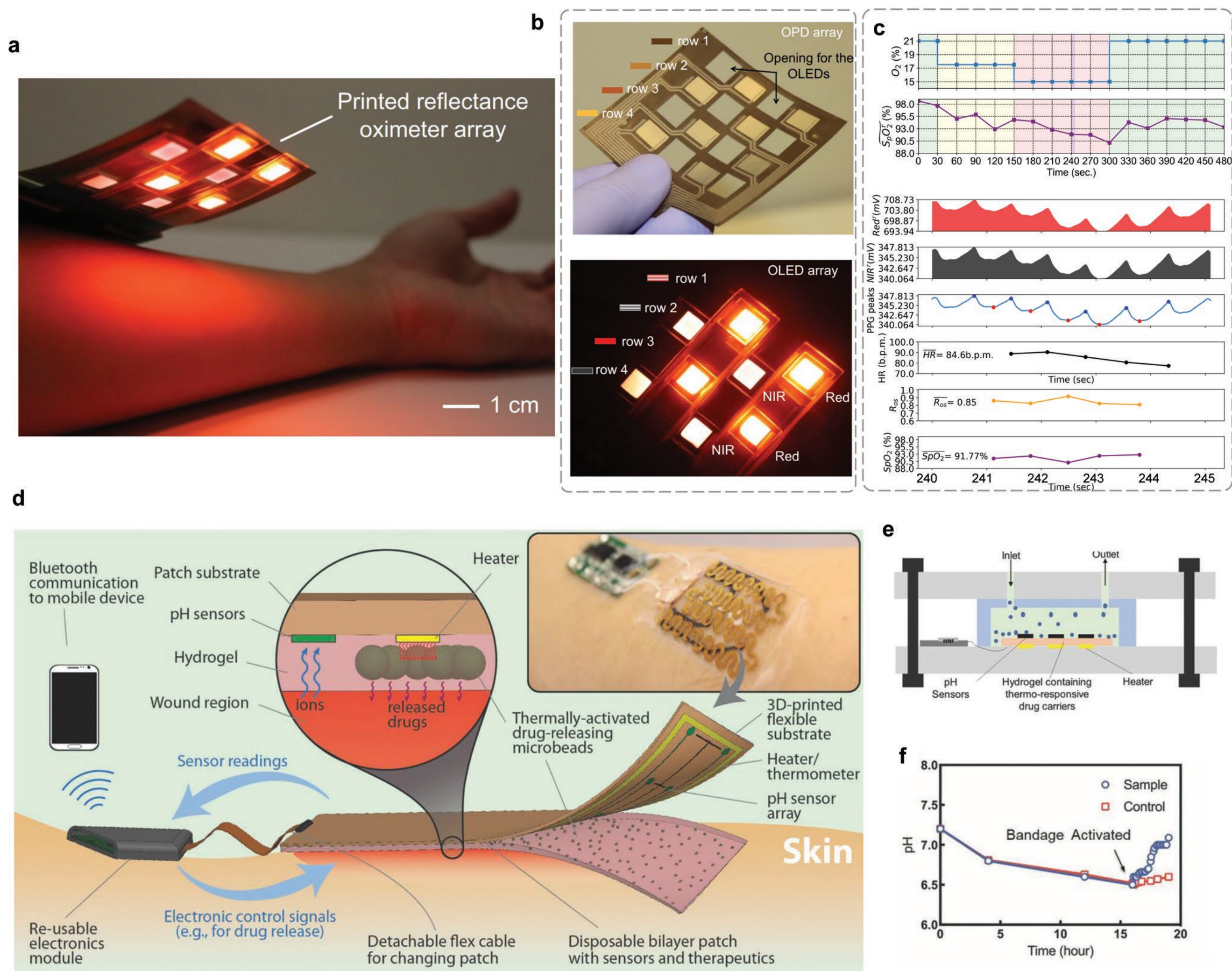

Figure 15. FHE systems for diagnostics and drug delivery. a) A flexible oximeter array composed of arrays of OLEDs and OPDs that measures oxygenation of blood and tissue. b) Printed OPD array that measures the reflected light, and red and near-infrared OLED arrays that are used as the light source. c) Change in pulse oxygenation of a volunteer measured using the oximeter array. The sensor accurately picked up the change in oxygenation from 98% to 90%. a–c) Reproduced with permission.[192] Copyright 2018, National Academy of Sciences. d) Schematic and conceptual view of a smart bandage that is composed of an array of flexible pH sensors and a flexible heater to trigger thermoresponsive drug carriers. In a closed-loop system, the thermoresponsive drug is released by the flexible heater when activated. e) Schematics of in vitro model for culturing of *S. aureus* bacteria in a bioreactor monitored with pH sensor and treated with the patch loaded with an antibiotic. f) In vitro test showing the pH variation over time, followed by the activation of the heater at pH = 6.5. d–f) Reproduced with permission.[193] Copyright 2019, Wiley-VCH.

Figure 16d, reported by Quintero et al. 2016.[62] This is a printed RFID label with an inkjet-printed multisensor platform for environmental monitoring. The platform can measure humidity, ammonia, and temperature. The printed platform was integrated after fabrication to the main RFID carrier, which contained an NFC RFID chip, a microprocessor, a readout frontend, screen-printed circuitry, and an antenna (Figure 16d,e). Flexible smart labels were introduced commercially by the company ThinFilm Electronics. They launched a hybrid printed temperature sensing label consisting of memory, display, and wireless interface (Figure 16f).

Another application area for FHE is precision agriculture. A few recent studies have shown the use of flexible and stretchable sensors in agricultural monitoring. Tang et al. printed a flexible strain sensor directly on the fruits using a chitosan-based ink.[217] These sensors provided good adhesion to the fruits and identified mechanical injuries to the fruits. Oren et al. reported a graphene-on-tape flexible sensor that can measure water flow through plants.[218] The sensor is developed by using drop-casting a graphene film on a prepatterned PDMS surface then transferring the patterned graphene surface onto a target tape. In another study, Nassar et al. demonstrated a flexible and stretchable device with multiple sensing capabilities for plant health monitoring.[64] The reported plant wearable is designed by integrating temperature, humidity, and strain sensors. The strain sensors were developed by depositing a thin gold metal film on top of PDMS substrate. The temperature and humidity sensors were fabricated on the same flexible and PI/PDMS platform. Zhao et al.

© 2019 WILEY-VCH Verlag GmbH & Co. KGaA, Weinheim

Table 4. Overview of the literature on printed sensors for environmental, industrial, and agricultural monitoring.

Signal	Measurement methods	Measurement range	Measurement sensitivity	Ref.
Temperature	Printed thermistor or embedded sensor in RFIC	−20 to 80 °C	1 °C	[62,134,198,199]
Humidity	Printed resistor and capacitor; antenna detuning; surface-mounted optical reflectometry	20–90% RH or binary configuration	1–9% R.H.	[62,112,134,150,198,200–207]
Gas (volatile chemicals, ammonia, oxygen, carbon monoxide, nitrogen dioxide)	Printed resistor and capacitor (with coating); antenna detuning; surface-mounted optical reflectometry	Gas dependent	Gas dependent	[62,112,148,201,208–211]
Liquid chemicals	Printed resistor and capacitor	Chemical dependent	Chemical dependent	[151,212,213]
Mechanical forces (pressure, deformation, and strain)	Printed resistor and capacitor (with coating); antenna detuning; surface-mounted sensors	–	–	[137,214,215]
Light (UV to IR)	Surface mounted PDs	–	–	[134]

also demonstrated a multifunctional agricultural monitoring sensor which can measure strain, impedance, temperature, and light intensity.[216] The sensor is fabricated by combining CMOS, printable electronics, and transfer printing techniques, leading to hydration, temperature, strain, and light illuminance sensing capabilities on leaves (**Figure 17**). Unlike other reported sensors

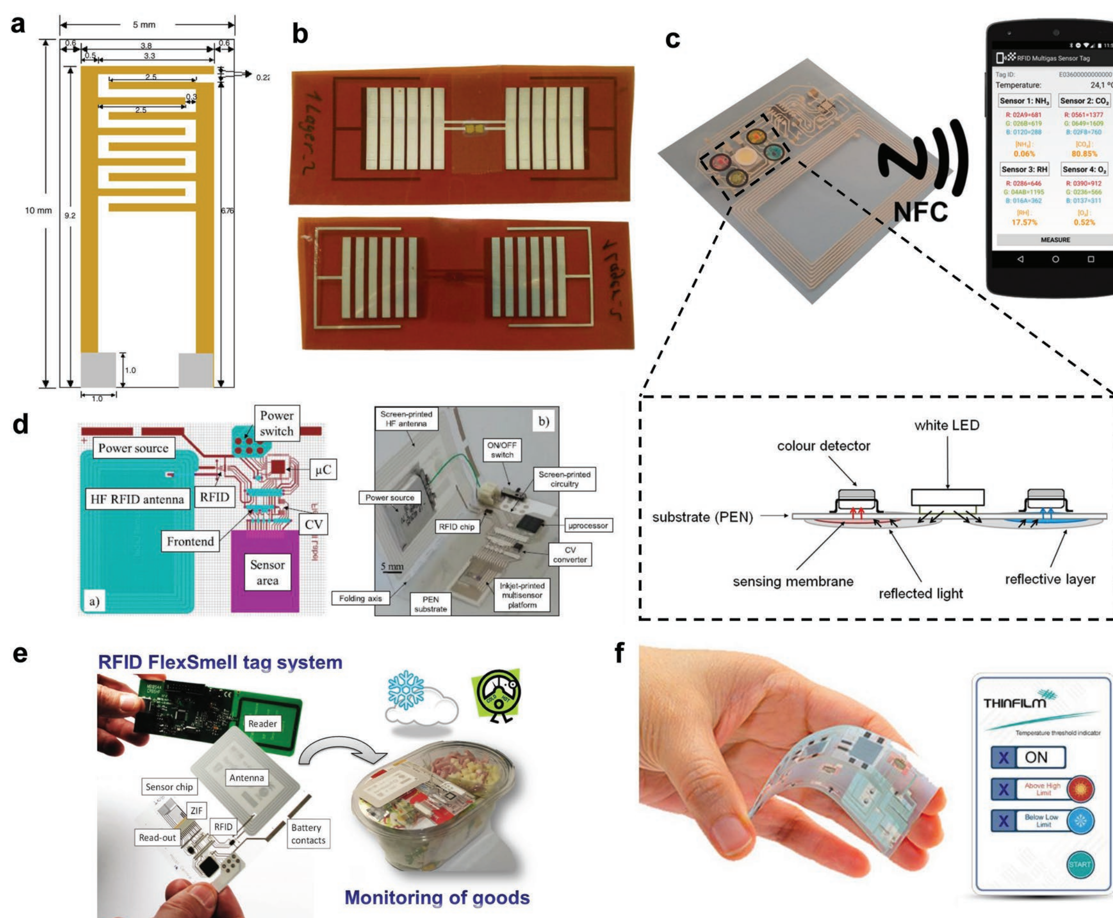

Figure 16. FHE systems in industrial and environmental monitoring. a) The layout of a printed, interdigitated electrode for humidity sensing (dimensions in mm). Reproduced with permission.[203] Copyright 2005, Elsevier. b) RFID antenna designed to function as a humidity sensor. Reproduced with permission.[207] Copyright 2011, IEEE. c) Wireless, printed multigas sensor using optical reflectometry. Reproduced with permission.[201] Copyright 2017, ACS Publications. d,e) Inkjet-printed multisensor platform for monitoring goods. d,e) Reproduced with permission.[62] Copyright 2016, IOP Publishing. f) A hybrid printed smart temperature sensing label consisting of memory, display, and wireless interface. Photo provided by and used with permission from ThinFilm Electronics.

 © 2019 WILEY-VCH Verlag GmbH & Co. KGaA, Weinheim

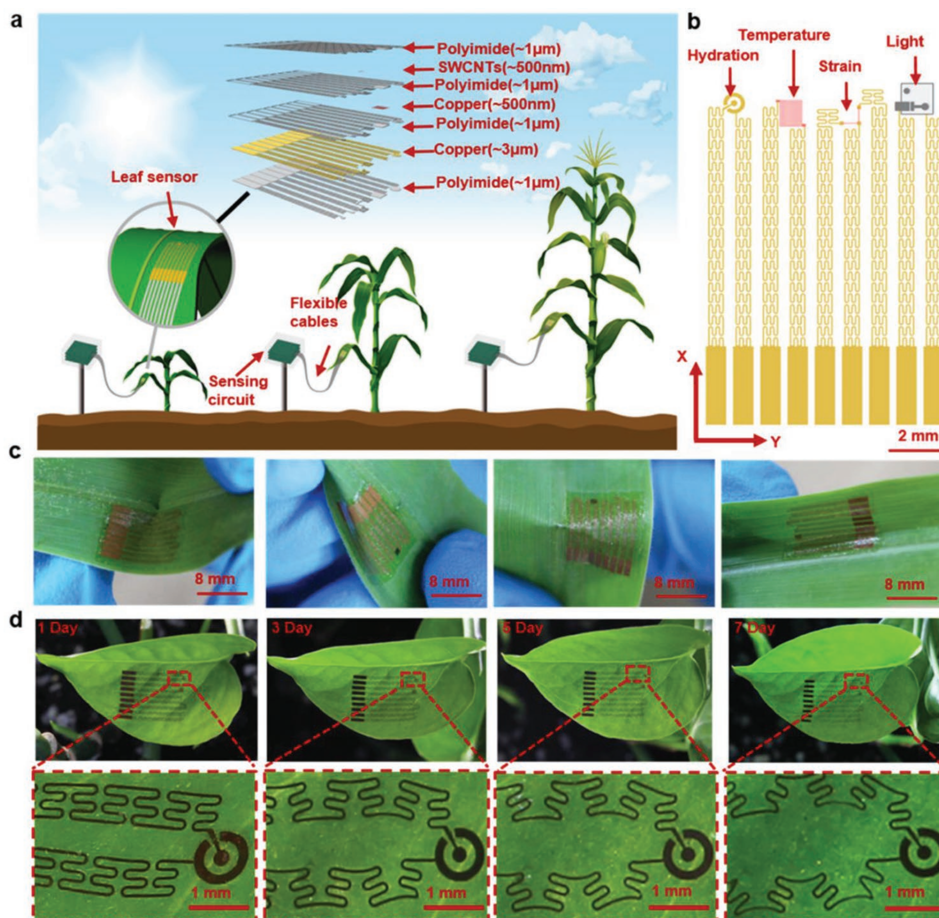

Figure 17. Schematics and demonstration of a multifunctional stretchable sensor on a leaf. a) Schematic diagram and exploded view of a leaf sensor. b) Top view of the leaf sensor. c) The sensor can adapt to the morphology of a corn leaf and deform together with the leaf. d) The sensor is attached on a leaf and grows together with the leaf throughout 7 days. a–d) Reproduced with permission.[216] Copyright 2019, ACS Publications.

these stretchable sensors can grow with the leaves making them compatible for long-term monitoring.

3.3. Structural Health Monitoring with FHE

Structural health monitoring (SHM) is an application domain that can be considerably benefited by FHE. Civil structures require sensors to be placed over an area to collect information from the structure—silicon electronics over large-area is not as cost-effective as the price of vacuum processing drastically increases with area scaling. On the other hand, FHE can be fabricated in roll-to-roll processes on flexible substrates, making them ideal for large-area SHM. SHM refers to the process of observing the response of a structure or a mechanical system over time in order to determine the current state of the structure's health. The earliest SHM involved visual inspection and tap-testing. With time, the SHM techniques have evolved, becoming more sensor dependent, especially in aerospace and mechanical industry. Civil infrastructures and buildings have not yet fully shifted to sensor-based SHM. However, recent years have seen a significant rise in instrumented structures.[235,236]

The main signals of interest in SHM are strain, acceleration, displacement, temperature, wind pressure, and corrosion. **Table 5** shows the different sensing methods that are employed for these parameters and the required measurement range for the civil SHM applications. Using these signals, damage detection methods are developed. A comprehensive review of all the damage detection methods is described by Doebling et al.[237] The methods are usually classified into two categories, local damage detection, and global damage detection. For example, strain, temperature, and corrosion measurements usually provide information on local damage. To get information of an entire large-scale structure using strain measurements only, a large amount of distributed strain gauges will be necessary, which will increase the cost of instrumentation. There are other sensing methods available for local damage detection which are noncontact such as ultrasonic inspection. However, to utilize such a method, trained personnel is required, rendering the method expensive. Hamburger reported that after the 1994 Northridge earthquake, welded connection inspection with ultrasonic methods reached $1000 per connection.[238] In all of the local damage detection method, some prior knowledge of damage proximity is necessary to install the sensors or carry out the inspection.[239]

 © 2019 WILEY-VCH Verlag GmbH & Co. KGaA, Weinheim

Table 5. Sensing parameters, methods, and measurement range for SHM.

Parameter	Sensing method	Measurement range	Ref.
Strain	Fiber Bragg grating	0.1–5000 $\mu\varepsilon^{b)}$	[219]
	Foil-type strain gauge$^{a)}$	1–40 000 $\mu\varepsilon$	[220]
	Semiconductor strain gauge$^{a)}$	0.25–3000 $\mu\varepsilon$	[221,222]
	Vibrating wire strain gauge	0.1–3000 $\mu\varepsilon$	[221]
Acceleration			
a) Earthquake acceleration	Seismometer, accelerometer	±4*g*	[223]
b) Ambient acceleration	Accelerometer	±0.5*g*	[224,225]
Displacement	Linear variable differential transducers (LVDT)	0.01–100 cm	[226]
	Fiber optic sensor	0.02–30 cm	[227]
	Global positioning system (GPS)	>0.5 cm	[228]
	Vision-based	>1 mm	[229]
Temperature	Thermocouple	−200 to 2600 °C	[221]
	Fiber optic sensor	−40 to 190 °C	[230]
	Thermistor$^{a)}$	−200 to 650 °C	[221]
	Thermography	−20 to 500 °C	[231]
Wind pressure	Anemometer	0–270 km h^{-1}	[232]
Corrosion	Corrosion sensor	–	[233]
	Fiber optic sensor	–	[221]
	Acoustic emission	–	[234]

$^{a)}$Fabricated using printing techniques; $^{b)}\mu\varepsilon$ = strain × 10^6.

The global damage detection methods provide damage condition of the entire structure. Acceleration measurements are usually used to extract dynamic characteristics (such as fundamental period/frequency, mode shape, etc.) and identify damage. Displacement values are also used to estimate global damage. However, the modal properties are affected by environmental and operational conditions[241] and have low sensitivity to local damage.[242] Researchers have shown other acceleration-based methods that are better global damage indicators than modal properties.[243,244] Moreover, the possibility of using acceleration measurement as local damage indicator has recently been shown.[245,246] Due to the high cost of conventional acceleration based SHM systems, nodal densities of such systems are usually low. Consequently, the monitoring resolution is negatively impacted.

The ideal SHM system would be the one that employs local and global systems simultaneously. Hong Kong's Tsing Ma suspension bridge has wind and structural health monitoring system (WASHM) which combines global and local sensing methods. It has 543 sensors comprising of accelerometers, strain gauges, displacement transducers, level sensors, anemometers, temperature sensors, and weigh-in-motion sensors, installed permanently on the bridges, and the data acquisition and processing system.[247,248] The cost of instrumentation is estimated to have exceeded $8 million[239] with cost per sensor $22 875. However, this large number of sensors with high instrumentation cost covered only certain sections of the bridge.

To address the limitations of current sensing technologies for large-scale SHM, the research community is actively exploring new technologies that can advance the current state-of-practice in SHM. FHE is one such technology. Printed electronics can be fabricated in roll-to-roll processes on flexible substrates, making them feasible and ideal for large-area SHM. Similar approaches can be utilized for monitoring the automotive, aeroplanes, and machinery. Here we discuss some examples of FHE that were used in civil infrastructure and aerospace monitoring.

Application of flexible sensors for civil structure monitoring is a fairly new concept. Flexible materials are so far mostly applied to develop strain sensors. Carbon nanotube (CNT) based thin films are primarily used for these sensors. An effective way of taking advantage of the unique material properties of CNT is to embed them in a flexible epoxy matrix as part of a fiber-reinforced polymer (FRP) composite. Hou et al. developed piezoresistive CNT-based thin film strain sensors with which distributed sensing was achieved.[249] Loh et al. successfully used this sensor to identify the location and severity of impact damage on an aluminum plate.[250] Zhang et al. also developed a piezoresistive strain sensor using an elastomeric composite film prepared with polyurethane and CNT.[251] This sensor was validated for 30% tensile strain making it comparable to the foil type strain sensors. Another strain sensor developed by Ryu et al. used inkjet printing for printing flexible polymer electrodes that enhanced fabrication scalability.[252] Load test on reinforced concrete sample showed the sensing range reaching 2% tensile strain. Zymelka et al. developed a low-cost graphite-based printed strain sensor array—with a temperature calibration, this sensor array can be used in different seasons.[65] The sensor array was used on a highway bridge for detecting formation of cracks (**Figure 18**a–c). They used screen printing technique to assemble the sensor array, with a linewidth of 150 µm (Figure 18d–f).[65,240]

Other than strain measurements, application of flexible sensors are reported for crack and corrosion monitoring. Spatial corrosion monitoring was demonstrated using sensors developed by Pyo et al.[66] Meyers et al. reported a thin film sensor that can generate and sense Lamb waves enabling detection of cracks in steel plates.[253]

Significant progress has been made in the field of aerospace health monitoring in terms of application of flexible sensors. The Structures and Composites Laboratory (SACL) at Stanford University has been developing bioinspired stretchable sensor networks. This network consists of extendable microwires and micronodes that can carry various sensors or processors.[254] Kopsaftopoulos et al. used such a network consisting of 148 microsensors on a prototype intelligent composite unmanned aerial vehicle (UAV) wing.[255] The effectiveness and accuracy of this stretchable network is the important first step toward "fly-by-feel" aerospace vehicles. Chen et al. developed a distributed strain gauge network for obtaining the strain distribution of a designated region on a target structure.[256] This stretchable

© 2019 WILEY-VCH Verlag GmbH & Co. KGaA, Weinheim

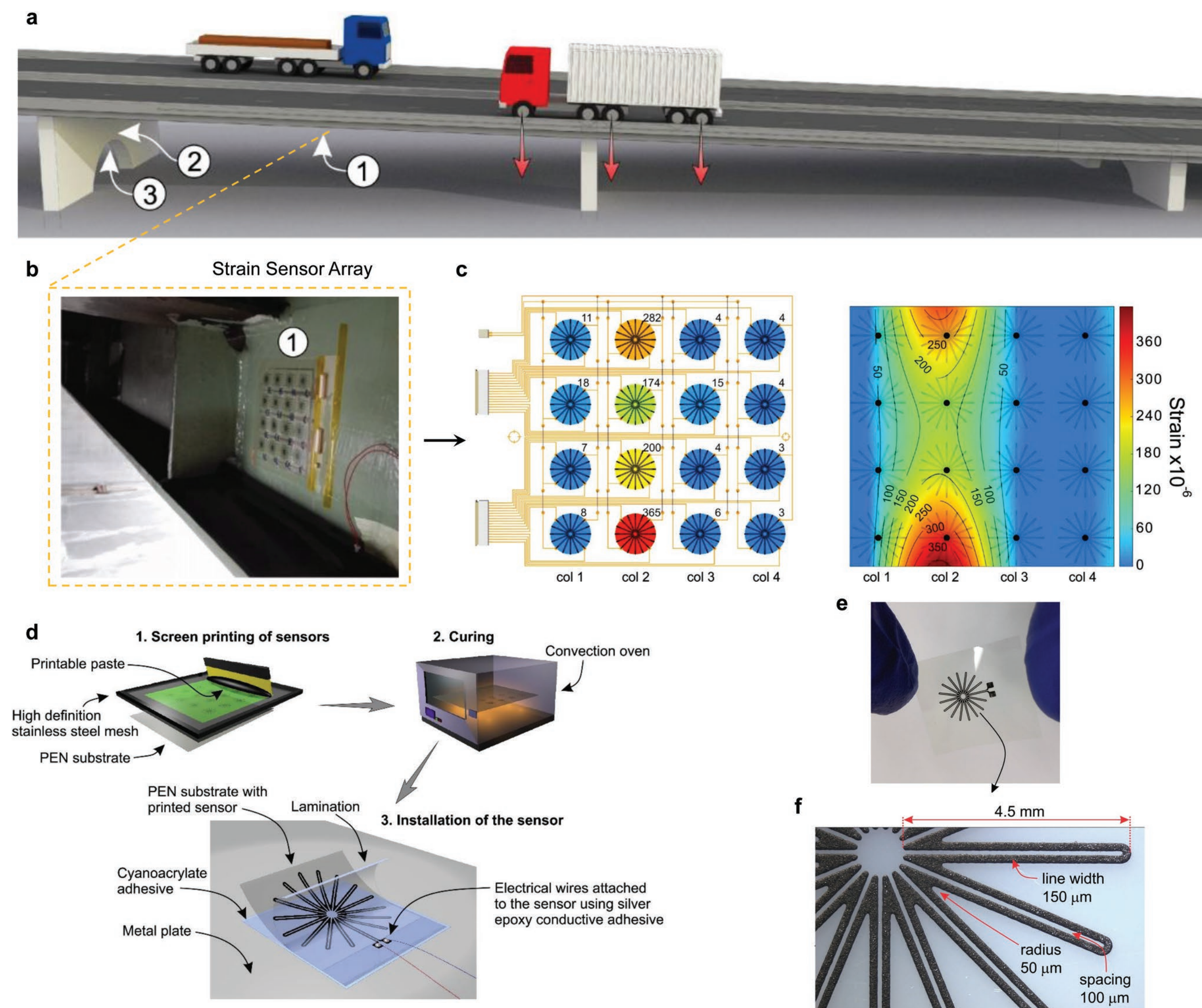

Figure 18. Printed strain sensor array used to detect damage in a highway bridge. a) Location of the sensor array. b) Sensor array on metal girder. c) Measurement from one array, showing crack formation. d) Schematic diagram of the sensor fabrication process. a–d) Reproduced with permission.[65] Copyright 2017, IOP Publishing. e) Photograph of a single strain sensor. f) Zoomed-in view of a sensors showing a linewidth of 150 µm and a spacing of 100 µm. e,f) Reproduced with permission.[240] Copyright 2017, Elsevier.

network had 27 strain gauges, 6 temperature devices, and 8 piezoelectric transducers. The network demonstrated the ability to conform to curved surfaces and provide reliable results. Xu et al. developed a shear stress sensor skin to monitor flow separation on the leading edge of UAVs.[257]

Printed sensors have also been utilized in monitoring of aerospace components. Zhang et al. inkjet printed silver nanoparticles on PET substrates to manufacture lightweight strain gauges for aerospace structures; the printed strain sensors achieve higher strain sensitivity and improved fatigue resistance.[258] Lee et al. also used printed sensors on glass fiber reinforced polymer (GFRP) and carbon fiber reinforced polymer (CFRP) coupons as strain gauges, whose gauge factor can be tuned by sensor geometry.[259] Zhao et al. developed and embedded an inkjet-printed CNT strain distribution sensing film at the interface between an adherend and the adhesive in a single-lap joint configuration to monitor the spatial strain distribution over the bonding area.[260] Bekas et al. developed a thin film consisting of an array of lead zirconate titanate (PZT) sensors and an inkjet-printed conductive network that can withstand variable operating conditions and harsh environment typically faced by aerospace structures.[67] The diagnostic film can be either surface mounted on a structure or embedded within a composite interlayer.

4. Reliability Testing of FHE

As application areas of FHE are growing, it is imperative to ensure reliable operation of the devices under environmental or physical stresses. Since FHE is still not a mature technology, there are not many reports in the literature on FHE reliability.

© 2019 WILEY-VCH Verlag GmbH & Co. KGaA, Weinheim

Here, we discuss the reliability testing that is needed to warrant an FHE lifetime of months to years.

One of the major challenges in FHE is the stability of the materials. Ideally, FHE materials should be soft, flexible, and stretchable. In comparison, existing electronics are rigid and hard, which ensures their robustness and good electronic performance. The mechanical requirements of flexibility and stretchability fundamentally oppose pristine electronic properties of printed electronics. Adding flexibility and stretchability to electronic materials degrades their electronic performance.[261] This is one of the biggest hurdles in designing materials for FHE.

Furthermore, printed electronics suffer from batch-to-batch and device-to-device process variability.[262] This variation directly influences FHE performance. If printed circuits are used in the design, minimizing device-to-device variability is essential to ensure adequate circuit operation. In a printed circuit composed of a few hundreds of transistors, variation in a single transistor will impede the overall performance. Due to the variability and low performance, only small modular circuits are currently printed in FHE systems, and the rest of the functionality is provided by silicon ICs.

Primarily, to ensure reliable operation, environmental and mechanical reliability testings are needed for FHE. Environmental tests involve thermal cycling or prolonged exposure to high temperature and humidity conditions. Accelerated lifetime testing, which is used in conventional silicon electronics, can also be adapted for FHE reliability testing. Mechanical tests involve studying bonding mechanisms, materials, and their reliability under bending, flexing, and twisting. Under repeated bending at a specified radius or shear force tests, the interfaces are examined between the rigid components and printed circuits lines. Soman et al. observed crack formation at the solder joints of silicon ICs with repeated bending (**Figure 19**).[54] In that study, optimizing a few design parameters helped the reliability of the device: 1) choosing the right combination of metal and flexible substrate thickness, 2) using a low-temperature solder, 3) adding strain compensations designs at the copper pad to silicon IC joints, and 4) using an inert metal for the printed to plated metal interface.

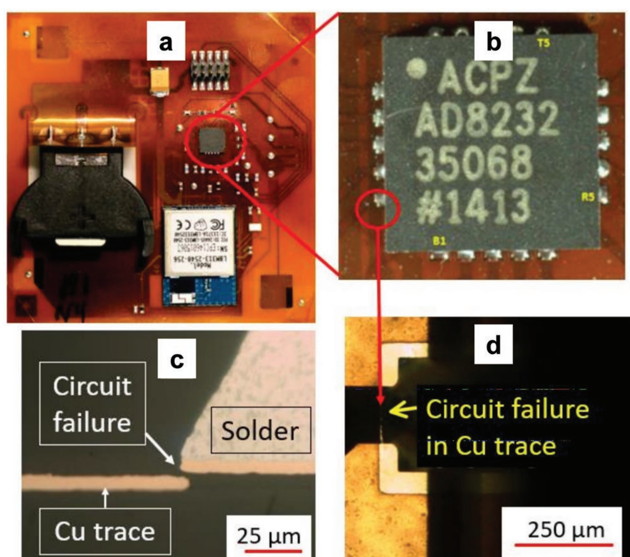

Figure 19. FHE device failure during reliability testing. a) A wearable sensor patch showing a silicon IC on a flexible substrate. b–d) Circuit failure at the flexible circuit and silicon IC interface due to crack formation. a–d) Reproduced with permission.[54] Copyright 2019, IEEE.

Since manufacturing is time-consuming and expensive, simulation tools can also be used to model and design different layers of the device stack as well as the complete device.[263] Overall, FHE materials and method are not as mature as silicon IC and conventional rigid circuit board industries. There is ample room for improvement in developing flexible materials, encapsulation, interconnects, which can vastly improve the reliability of the devices.

5. Conclusion and Outlook

While the outlook for FHE is extremely promising, many challenges still persist. At the materials level, FHE needs materials that are soft, flexible, and stretchable. These properties are at odds with traditional silicon-based electronics. Organic and inorganic nanomaterials are promising for FHE. In the past few years, researchers around the world have shown fascinating plastic and elastomeric soft materials that can be adapted for FHE. However, further research and development are required for improving the stability and performance of these inherently soft materials.

On the printed electronics side, advanced printing techniques are required that can produce reliable and reproducible printed features. Recently, high-speed and roll-to-roll methods have been developed to print high-performance transistors. However, process variability remains a challenge. The process variability should be minimized, in particular, when fabricating transistors for circuit applications. In terms of integration of printed electronics to silicon ICs, a fast assembly and bonding process would be ideal for large-scale manufacturing. Also, innovations are needed in conductive and nonconductive adhesives that are inherently flexible and compatible with FHE processes.

Conventionally semiconductor processing is a bit constrained, because vacuum processing is expensive and scaling to large areas is even more challenging. Flexible and printed sensors are most-suited for large-scale sensing. The cost, form factor and fabrication of printed electronics are a perfect match for medical/environment/agricultural/structural sensing. Coupled with silicon ICs, these devices will provide the ideal sensing platform. Silicon ICs will remain the key technology for data processing and communication, because of their unparalleled performance advantage. Therefore, FHE will be the balance of the two fields.

Recently, impressive advancement has happened in the field of skin-inspired stretchable electronics.[6,8,48,95] These electronics are thin, light, and comfortable—in essence, "imperceptible." In the near future, we can except imperceptible wearable electronics—the wearer will not even feel the wearable after putting on the device. The wearable will act as a "second skin," and will be able to relay sensory information such as touch and temperature. Even further, the wearable will be able to monitor vital signs and analytes in bodily fluids for health monitoring—this

© 2019 WILEY-VCH Verlag GmbH & Co. KGaA, Weinheim

is the vision for future wearables. Flexible and stretchable hybrid electronics is a vital technology to realize this vision.

We envision in the next 10 years, the emerging field of FHE will grow not in just academic but also in industrial research. New and exciting areas such as wearable electronics, soft robotics, ubiquitous large-area sensing will also directly benefit from FHE implementations.

Acknowledgements

This work was partially supported by Intel Corporation via Semiconductor Research Corporation Grant No. 2014-IN-2571, Cambridge Display Technology Limited (Company Number 02672530), and FlexTech under contract AFOSR-42299. A.T. wishes to acknowledge support from the FWO [PEGASUS]2 Marie Sklodowska-Curie Fellowship.

Conflict of Interest

The authors declare no conflict of interest.

Keywords

environmental sensors, flexible electronics, printed electronics, structural health monitoring, wearable health monitoring

Received: August 15, 2019
Revised: September 8, 2019
Published online:

[1] W. S. Wong, M. L. Chabinyc, T.-N. Ng, A. Salleo, *Flexible Electronics: Materials and Applications*, Springer, New York **2009**, pp. 143–181.
[2] J. A. Rogers, T. Someya, Y. Huang, *Science* **2010**, *327*, 1603.
[3] A. C. Arias, J. D. MacKenzie, I. McCulloch, J. Rivnay, A. Salleo, *Chem. Rev.* **2010**, *110*, 3.
[4] M. L. Hammock, A. Chortos, B. C. Tee, J. B. Tok, Z. Bao, *Adv. Mater.* **2013**, *25*, 5997.
[5] T. R. Ray, J. Choi, A. J. Bandodkar, S. Krishnan, P. Gutruf, L. Tian, R. Ghaffari, J. A. Rogers, *Chem. Rev.* **2019**, *119*, 5461.
[6] H. Xu, L. Yin, C. Liu, X. Sheng, N. Zhao, *Adv. Mater.* **2018**, *30*, 1800156.
[7] Y. Khan, A. E. Ostfeld, C. M. Lochner, A. Pierre, A. C. Arias, *Adv. Mater.* **2016**, *28*, 4373.
[8] S. Choi, H. Lee, R. Ghaffari, T. Hyeon, D. Kim, *Adv. Mater.* **2016**, *28*, 4203.
[9] S. F. Shaikh, H. F. Mazo-Mantilla, N. Qaiser, S. M. Khan, J. M. Nassar, N. R. Geraldi, C. M. Duarte, M. M. Hussain, *Small* **2019**, *15*, 1804385.
[10] S. M. Khan, S. F. Shaikh, N. Qaiser, M. M. Hussain, *IEEE Trans. Electron Devices* **2018**, *65*, 2892.
[11] M. Berggren, D. Nilsson, N. D. Robinson, *Nat. Mater.* **2007**, *6*, 3.
[12] A. Kamyshny, S. Magdassi, *Small* **2014**, *10*, 3515.
[13] J. Perelaer, P. J. Smith, D. Mager, D. Soltman, S. K. Volkman, V. Subramanian, J. G. Korvink, U. S. Schubert, *J. Mater. Chem.* **2010**, *20*, 8446.
[14] J. A. Lewis, B. Y. Ahn, *Nature* **2015**, *518*, 42.
[15] A. E. Ostfeld, I. Deckman, A. M. Gaikwad, C. M. Lochner, A. C. Arias, *Sci. Rep.* **2015**, *5*, 15959.
[16] G. Grau, J. Cen, H. Kang, R. Kitsomboonloha, W. J. Scheideler, V. Subramanian, *Flexible Printed Electron.* **2016**, *1*, 023002.
[17] N. Palavesam, S. Marin, D. Hemmetzberger, C. Landesberger, K. Bock, C. Kutter, *Flexible Printed Electron.* **2018**, *3*, 014002.
[18] W. Clemens, W. Fix, J. Ficker, A. Knobloch, A. Ullmann, *J. Mater. Res.* **2004**, *19*, 1963.
[19] S. G. Bucella, A. Luzio, E. Gann, L. Thomsen, C. R. McNeill, G. Pace, A. Perinot, Z. Chen, A. Facchetti, M. Caironi, *Nat. Commun.* **2015**, *6*, 8394.
[20] S. Lin, X. Bai, H. Wang, H. Wang, J. Song, K. Huang, C. Wang, N. Wang, B. Li, M. Lei, H. Wu, *Adv. Mater.* **2017**, *29*, 1703238.
[21] H. Koo, W. Lee, Y. Choi, J. Sun, J. Bak, J. Noh, V. Subramanian, Y. Azuma, Y. Majima, G. Cho, *Sci. Rep.* **2015**, *5*, 14459.
[22] S.-P. Chen, H.-L. Chiu, P.-H. Wang, Y.-C. Liao, *ECS J. Solid State Sci. Technol.* **2015**, *4*, P3026.
[23] Y. Khan, F. J. Pavinatto, M. C. Lin, A. Liao, S. L. Swisher, K. Mann, V. Subramanian, M. M. Maharbiz, A. C. Arias, *Adv. Funct. Mater.* **2016**, *26*, 1004.
[24] J. Li, W. Tang, Q. Wang, W. Sun, Q. Zhang, X. Guo, X. Wang, F. Yan, *Mater. Sci. Eng., R* **2018**, *127*, 1.
[25] A. M. Gaikwad, Y. Khan, A. E. Ostfeld, S. Pandya, S. Abraham, A. C. Arias, *Org. Electron.* **2016**, *30*, 18.
[26] S. K. Garlapati, M. Divya, B. Breitung, R. Kruk, H. Hahn, S. Dasgupta, *Adv. Mater.* **2018**, *30*, 1707600.
[27] W. J. Scheideler, R. Kumar, A. R. Zeumault, V. Subramanian, *Adv. Funct. Mater.* **2017**, *27*, 1606062.
[28] C. Sekine, Y. Tsubata, T. Yamada, M. Kitano, S. Doi, *Sci. Technol. Adv. Mater.* **2014**, *15*, 034203.
[29] A. Pierre, M. Sadeghi, M. M. Payne, A. Facchetti, J. E. Anthony, A. C. Arias, *Adv. Mater.* **2014**, *26*, 5722.
[30] H. Kang, R. Kitsomboonloha, K. Ulmer, L. Stecker, G. Grau, J. Jang, V. Subramanian, *Org. Electron.* **2014**, *15*, 3639.
[31] J. S. Chang, A. F. Facchetti, R. Reuss, *IEEE J. Emerging Sel. Top. Circuits Syst.* **2017**, *7*, 7.
[32] M. G. Mohammed, R. Kramer, *Adv. Mater.* **2017**, *29*, 1604965.
[33] X. Wang, J. Liu, *Micromachines* **2016**, *7*, 206.
[34] V. Subramanian, J. Cen, A. d. l. F. Vornbrock, G. Grau, H. Kang, R. Kitsomboonloha, D. Soltman, H.-Y. Tseng, *Proc. IEEE* **2015**, *103*, 567.
[35] W. J. Hyun, E. B. Secor, M. C. Hersam, C. D. Frisbie, L. F. Francis, *Adv. Mater.* **2015**, *27*, 109.
[36] T. N. Ng, D. E. Schwartz, L. L. Lavery, G. L. Whiting, B. Russo, B. Krusor, J. Veres, P. Bröms, L. Herlogsson, N. Alam, O. Hagel, J. Nilsson, C. Karlsson, *Sci. Rep.* **2012**, *2*, 585.
[37] C.-M. Lai, Y.-H. Yeh, Y.-H. Huang, *US Patent App. 11/308, 015*, **2007**.
[38] S. Reineke, F. Lindner, G. Schwartz, N. Seidler, K. Walzer, B. Lüssem, K. Leo, *Nature* **2009**, *459*, 234.
[39] T. Sekitani, H. Nakajima, H. Maeda, T. Fukushima, T. Aida, K. Hata, T. Someya, *Nat. Mater.* **2009**, *8*, 494.
[40] F. Zare Bidoky, B. Tang, R. Ma, K. S. Jochem, W. J. Hyun, D. Song, S. J. Koester, T. P. Lodge, C. D. Frisbie, *Adv. Funct. Mater.*, https://doi.org/10.1002/adfm.201902028.
[41] J. Kwon, Y. Takeda, R. Shiwaku, S. Tokito, K. Cho, S. Jung, *Nat. Commun.* **2019**, *10*, 54.
[42] R. Rahimi, M. Ochoa, T. Parupudi, X. Zhao, I. K. Yazdi, M. R. Dokmeci, A. Tamayol, A. Khademhosseini, B. Ziaie, *Sens. Actuators, B* **2016**, *229*, 609.
[43] K. Chen, W. Gao, S. Emaminejad, D. Kiriya, H. Ota, H. Y. Y. Nyein, K. Takei, A. Javey, *Adv. Mater.* **2016**, *28*, 4397.
[44] G. Mattana, D. Briand, *Mater. Today* **2016**, *19*, 88.
[45] R. A. Street, T. N. Ng, D. E. Schwartz, G. L. Whiting, J. P. Lu, R. D. Bringans, J. Veres, *Proc. IEEE* **2015**, *103*, 607.
[46] Y. Khan, D. Han, J. Ting, M. Ahmed, R. Nagisetty, A. C. Arias, *IEEE Access* **2019**, *7*, 128114.

© 2019 WILEY-VCH Verlag GmbH & Co. KGaA, Weinheim

[47] Y. Zheng, Z. He, Y. Gao, J. Liu, *Sci. Rep.* **2013**, *3*, srep01786.
[48] C. Zhu, A. Chortos, Y. Wang, R. Pfattner, T. Lei, A. C. Hinckley, I. Pochorovski, X. Yan, J. W.-F. To, J. Y. Oh, J. B.-H. Tok, Z. Bao, B. Murmann, *Nat. Electron.* **2018**, *1*, 183.
[49] Y. Kim, H. Kim, H.-J. Yoo, *IEEE Trans. Adv. Packag.* **2010**, *33*, 857.
[50] D. Zhong, Z. Zhang, L. Ding, J. Han, M. Xiao, J. Si, L. Xu, C. Qiu, L.-M. Peng, *Nat. Electron.* **2018**, *1*, 40.
[51] I. McCulloch, M. Heeney, C. Bailey, K. Genevicius, I. MacDonald, M. Shkunov, D. Sparrowe, S. Tierney, R. Wagner, W. Zhang, M. L. Chabinyc, R. J. Kline, M. D. McGehee, M. F. Toney, *Nat. Mater.* **2006**, *5*, 328.
[52] M. Poliks, J. Turner, K. Ghose, Z. Jin, M. Garg, Q. Gui, A. Arias, Y. Kahn, M. Schadt, F. Egitto, in *2016 IEEE 66th Electronic Components and Technology Conf. (ECTC)*, IEEE, Piscataway, NJ, USA **2016**, p. 1623.
[53] Y. Khan, M. Garg, Q. Gui, M. Schadt, A. Gaikwad, D. Han, N. A. D. Yamamoto, P. Hart, R. Welte, W. Wilson, S. Czarnecki, M. Poliks, Z. Jin, K. Ghose, F. Egitto, J. Turner, A. C. Arias, *Adv. Funct. Mater.* **2016**, *26*, 8764.
[54] V. Soman, Y. Khan, M. Zabran, M. Schadt, P. Hart, M. Shay, F. Egitto, K. Papathomas, N. A. D. Yamamoto, D. Han, A. C. Arias, K. Ghose, M. D. Poliks, J. N. Turner, *IEEE Trans. Compon., Packag., Manuf. Technol.* **2019**, *9*, 1.
[55] R. A. Street, P. Mei, B. Krusor, S. E. Ready, Y. Zhang, D. E. Schwartz, A. Pierre, S. E. Doris, B. Russo, S. Kor, J. Veres, *Proc. SPIE* **2017**, *10366*, 103660C.
[56] T.-C. J. Huang, J. Marsh, S. H. Goodwin, D. S. Temple, in *2018 IEEE 36th VLSI Test Symp. (VTS)*, IEEE, Piscataway, NJ, USA **2018**, p. 1, https://doi.org/10.1109/VTS.2018.8368668.
[57] K. Xu, Y. Lu, K. Takei, *Adv. Mater. Technol.* **2019**, *4*, 1800628.
[58] Y. Ma, Y. Zhang, S. Cai, Z. Han, X. Liu, F. Wang, Y. Cao, Z. Wang, H. Li, Y. Chen, *Adv. Mater.*, https://doi.org/10.1002/adma.201902062.
[59] K. Kim, B. Kim, C. H. Lee, *Adv. Mater.*, https://doi.org/10.1002/adma.201902051.
[60] Y. Gao, L. Yu, J. C. Yeo, C. T. Lim, *Adv. Mater.*, https://doi.org/10.1002/adma.201902133.
[61] H.-R. Lim, H. S. Kim, R. Qazi, Y.-T. Kwon, J.-W. Jeong, W.-H. Yeo, *Adv. Mater.* **2019**, 1901924.
[62] A. V. Quintero, F. Molina-Lopez, E. Smits, E. Danesh, J. van den Brand, K. Persaud, A. Oprea, N. Barsan, U. Weimar, N. De Rooij, *Flexible Print. Electron.* **2016**, *1*, 025003.
[63] P. Escobedo, M. M. Erenas, N. L. Ruiz, M. A. Carvajal, S. G. Chocano, I. d. Orbe-Payá, L. F. Capitan-Vallvey, A. J. Palma, A. M. Olmos, *Anal. Chem.* **2017**, *89*, 1697.
[64] J. M. Nassar, S. M. Khan, D. R. Villalva, M. M. Nour, A. S. Almuslem, M. M. Hussain, *npj Flexible Electron.* **2018**, *2*, 24.
[65] D. Zymelka, K. Togashi, R. Ohigashi, T. Yamashita, S. Takamatsu, T. Itoh, T. Kobayashi, *Smart Mater. Struct.* **2017**, *26*, 105040.
[66] S. Pyo, K. J. Loh, T.-C. Hou, E. Jarva, J. P. Lynch, *Smart Struct. Syst.* **2011**, *8*, 139.
[67] D. G. Bekas, Z. Sharif-Khodaei, M. F. Aliabadi, *Sensors* **2018**, *18*, 2084.
[68] R. Das, X. He, K. Ghaffarzadeh, *Flexible, Printed and Organic Electronics 2019–2029: Forecasts, Players & Opportunities,* IDTechEx Research, Cambridge, UK **2018**.
[69] K. Suganuma, *Introduction to Printed Electronics*, Vol. *74*, Springer Science & Business Media, New York **2014**.
[70] P.-Y. Jar, R. Shanks, *J. Polym. Sci., Part B: Polym. Phys.* **1996**, *34*, 707.
[71] K. Okomori, T. Enomae, F. Onabe, *J. Pulp Pap. Sci.* **2001**, *27*, 262.
[72] D. Cai, A. Neyer, R. Kuckuk, H. Heise, *Opt. Mater.* **2008**, *30*, 1157.
[73] Z. Wang, A. A. Volinsky, N. D. Gallant, *J. Appl. Polym. Sci.* **2014**, *131*, 22.
[74] J. Corea, P. Ye, D. Seo, K. Butts-Pauly, A. C. Arias, M. Lustig, *Sci. Rep.* **2018**, *8*, 3392.
[75] G. Grau, R. Kitsomboonloha, S. L. Swisher, H. Kang, V. Subramanian, *Adv. Funct. Mater.* **2014**, *24*, 5067.
[76] J. Bang, W. S. Lee, B. Park, H. Joh, H. K. Woo, S. Jeon, J. Ahn, C. Jeong, T.-i. Kim, S. J. Oh, *Adv. Funct. Mater.* **2019**, *29*, 1903047.
[77] S. L. Swisher, S. K. Volkman, V. Subramanian, *ACS Appl. Mater. Interfaces* **2015**, *7*, 10069.
[78] F. C. Krebs, *Sol. Energy Mater. Sol. Cells* **2009**, *93*, 394.
[79] M. Välimäki, P. Apilo, R. Po, E. Jansson, A. Bernardi, M. Ylikunnari, M. Vilkman, G. Corso, J. Puustinen, J. Tuominen, *Nanoscale* **2015**, *7*, 9570.
[80] A. J. Heeger, E. B. Namdas, N. S. Sariciftci, *Semiconducting and Metallic Polymers*, Oxford University Press, Oxford **2010**.
[81] D. Han, Y. Khan, J. Ting, S. M. King, N. Yaacobi-Gross, M. J. Humphries, C. J. Newsome, A. C. Arias, *Adv. Mater.* **2017**, *29*, 1606206.
[82] D. Han, Y. Khan, K. Gopalan, A. Pierre, A. C. Arias, *Adv. Funct. Mater.* **2018**, *28*, 1802986.
[83] A. Pierre, I. Deckman, P. B. Lechêne, A. C. Arias, *Adv. Mater.* **2015**, *27*, 6411.
[84] B. P. Lechêne, M. Cowell, A. Pierre, J. W. Evans, P. K. Wright, A. C. Arias, *Nano Energy* **2016**, *26*, 631.
[85] Y. Aleeva, B. Pignataro, *J. Mater. Chem. C* **2014**, *2*, 6436.
[86] H. C. Nallan, J. A. Sadie, R. Kitsomboonloha, S. K. Volkman, V. Subramanian, *Langmuir* **2014**, *30*, 13470.
[87] A. Kamyshny, M. Ben-Moshe, S. Aviezer, S. Magdassi, *Macromol. Rapid Commun.* **2005**, *26*, 281.
[88] M. Singh, H. M. Haverinen, P. Dhagat, G. E. Jabbour, *Adv. Mater.* **2010**, *22*, 673.
[89] A. Ostfeld, *Ph.D. thesis*, University of California, **2016**.
[90] F. Molina-Lopez, T. Gao, U. Kraft, C. Zhu, T. Öhlund, R. Pfattner, V. Feig, Y. Kim, S. Wang, Y. Yun, *Nat. Commun.* **2019**, *10*, 2676.
[91] A. Thielens, I. Deckman, R. Aminzadeh, A. C. Arias, J. M. Rabaey, *IEEE Access* **2018**, *6*, 62050.
[92] H. Ota, S. Emaminejad, Y. Gao, A. Zhao, E. Wu, S. Challa, K. Chen, H. M. Fahad, A. K. Jha, D. Kiriya, *Adv. Mater. Technol.* **2016**, *1*, 1600013.
[93] A. D. Valentine, T. A. Busbee, J. W. Boley, J. R. Raney, A. Chortos, A. Kotikian, J. D. Berrigan, M. F. Durstock, J. A. Lewis, *Adv. Mater.* **2017**, *29*, 1703817.
[94] Z. Chen, S. N. Obaid, L. Lu, *Opt. Mater. Express* **2019**, *9*, 3843.
[95] S. Wang, J. Xu, W. Wang, G.-J. N. Wang, R. Rastak, F. Molina-Lopez, J. W. Chung, S. Niu, V. R. Feig, J. Lopez, *Nature* **2018**, *555*, 83.
[96] S. Gupta, W. T. Navaraj, L. Lorenzelli, R. Dahiya, *npj Flexible Electron.* **2018**, *2*, 8.
[97] J. P. Rojas, G. A. T. Sevilla, M. T. Ghoneim, S. B. Inayat, S. M. Ahmed, A. M. Hussain, M. M. Hussain, *ACS Nano* **2014**, *8*, 1468.
[98] R. L. Chaney, D. G. Wilson, D. R. Hackler, K. J. DeGregorio, D. E. Leber, in *2017 IEEE Workshop on Microelectronics and Electron Devices (WMED)*, IEEE, Piscataway, NJ, USA **2017**, pp. 1–4, https://doi.org/10.1109/WMED.2017.7916930.
[99] E. A. Angelopoulos, A. Kaiser, in *Ultra-thin Chip Technology and Applications*,Springer, New York **2011**, pp. 53–60.
[100] M. Zimmermann, J. N. Burghartz, W. Appel, C. Harendt, in *Ultra-thin Chip Technology and Applications*, Springer, New York **2011**, pp. 69–77.
[101] J. N. Burghartz, in *Ultra-thin Chip Technology and Applications*, Springer, New York **2011**, pp. 61–67.
[102] J. Niittynen, J. Kiilunen, J. Putaala, V. Pekkanen, M. Mäntysalo, H. Jantunen, D. Lupo, *Microelectron. Reliab.* **2012**, *52*, 2709.
[103] C. Harendt, J. Kostelnik, A. Kugler, E. Lorenz, S. Saller, A. Schreivogel, Z. Yu, J. N. Burghartz, *Solid-State Electron.* **2015**, *113*, 101.
[104] J. N. Burghartz, E. Angelopoulos, W. Appel, S. Endler, S. Ferwana, C. Harendt, M.-U. Hassan, H. Rempp, H. Richter,

 © 2019 WILEY-VCH Verlag GmbH & Co. KGaA, Weinheim

M. Zimmermann, in *2013 IEEE Int. Conf. of Electron Devices and Solid-state Circuits*, IEEE, Piscataway, NJ, USA **2013**, p. 1, https://doi.org/10.1109/EDSSC.2013.6628168.
[105] C. Linghu, S. Zhang, C. Wang, J. Song, *npj Flexible Electron.* **2018**, *2*, 26.
[106] C. Linghu, C. Wang, N. Cen, J. Wu, Z. Lai, J. Song, *Soft Matter* **2019**, *15*, 30.
[107] Y. Huang, H. Wu, L. Xiao, Y. Duan, H. Zhu, J. Bian, D. Ye, Z. Yin, *Mater. Horiz.* **2019**, *6*, 642.
[108] I. Mir, D. Kumar, *Int. J. Adhes. Adhes.* **2008**, *28*, 362.
[109] H. A. Andersson, A. Manuilskiy, S. Haller, M. Hummelgård, J. Sidén, C. Hummelgård, H. Olin, H.-E. Nilsson, *Nanotechnology* **2014**, *25*, 094002.
[110] J. Arrese, G. Vescio, E. Xuriguera, B. Medina-Rodriguez, A. Cornet, A. Cirera, *J. Appl. Phys.* **2017**, *121*, 104904.
[111] M. Ben Salah Ep Akin, *Master's thesis*, University of California, **2014**.
[112] R. Vyas, V. Lakafosis, H. Lee, G. Shaker, L. Yang, G. Orecchini, A. Traille, M. M. Tentzeris, L. Roselli, *IEEE Sens. J.* **2011**, *11*, 3139.
[113] L. Song, A. C. Myers, J. J. Adams, Y. Zhu, *ACS Appl. Mater. Interfaces* **2014**, *6*, 4248.
[114] J. G. Hester, S. Kim, J. Bito, T. Le, J. Kimionis, D. Revier, C. Saintsing, W. Su, B. Tehrani, A. Traille, B. S. Cook, M. M. Tentzeris, *Proc. IEEE* **2015**, *103*, 583.
[115] D. Godlinski, R. Zichner, V. Zöllmer, R. Baumann, *IET Microwaves, Antennas Propag.* **2017**, *11*, 2010.
[116] A. Rida, L. Yang, R. Vyas, M. Tentzeris, *IEEE Antennas Propag. Mag.* **2009**, *51*, 13.
[117] L. Yang, A. Rida, R. Vyas, M. M. Tentzeris, *IEEE Trans. Microwave Theory Tech.* **2007**, *55*, 2894.
[118] Z. Zhang, X. Zhang, Z. Xin, M. Deng, Y. Wen, Y. Song, *Nanotechnology* **2011**, *22*, 425601.
[119] H. F. Abutarboush, A. Shamim, in *2013 7th European Conference on Antennas and Propagation (EuCAP)*, IEEE, Piscataway, NJ, USA **2013**, pp. 3099–3102.
[120] L. Yang, R. Zhang, D. Staiculescu, C. P. Wong, M. M. Tentzeris, *IEEE Antennas Wireless Propag. Lett.* **2009**, *8*, 653.
[121] H. F. Abutarboush, A. Shamim, *IEEE Antennas Wireless Propag. Lett.* **2012**, *11*, 1234.
[122] S. Ahmed, F. A. Tahir, A. Shamim, H. M. Cheema, *IEEE Antennas Wireless Propag. Lett.* **2015**, *14*, 1802.
[123] H. Sillanpää, E. Halonen, T. Liimatta, M. Mäntysalo, in *2014 Int. Conf. on Electronics Packaging (ICEP)*, IEEE, Piscataway, NJ, USA **2014**, pp. 322–325.
[124] S. Kim, Y.-J. Ren, H. Lee, A. Rida, S. Nikolaou, M. M. Tentzeris, *IEEE Antennas Wireless Propag. Lett.* **2012**, *11*, 663.
[125] H. R. Khaleel, H. M. Al-Rizzo, D. G. Rucker, Y. Al-Naiemy, in *2011 IEEE Int. Symp. on Antennas and Propagation and USNC/URSI National Radio Science Meeting (AP-S/URSI 2011)*, IEEE, Piscataway, NJ, USA **2011**, https://doi.org/10.1109/APS.2011.5996536.
[126] H. R. Raad, A. I. Abbosh, H. M. Al-Rizzo, D. G. Rucker, *IEEE Trans. Antennas Propag.* **2013**, *61*, 524.
[127] A. A. Babar, J. Virtanen, V. A. Bhagavati, L. Ukkonen, A. Z. Elsherbeni, P. Kallio, L. Sydanheimo, in *2012 IEEE/MTT-S Int. Microwave Symp. Digest*, IEEE, Piscataway, NJ, USA **2012**, pp. 1–3, https://doi.org/10.1109/MWSYM.2012.6259566.
[128] S. M. Saeed, C. A. Balanis, C. R. Birtcher, *IEEE Antennas Wireless Propag. Lett.* **2016**, *15*, 1979.
[129] H. Subbaraman, D. T. Pham, X. Xu, M. Y. Chen, A. Hosseini, X. Lu, R. T. Chen, *IEEE Antennas Wireless Propag. Lett.* **2013**, *12*, 170.
[130] D. T. Pham, H. Subbaraman, M. Y. Chen, X. Xu, R. T. Chen, *IEEE Trans. Antennas Propag.* **2011**, *59*, 4553.
[131] D.-Y. Shin, Y. Lee, C. H. Kim, *Thin Solid Films* **2009**, *517*, 6112.
[132] L. Wang, Y.-X. Guo, B. Salam, L. C. W. Albert, in *2012 IEEE Asia-Pacific Conf. on Antennas and Propagation*, IEEE, Piscataway, NJ, USA **2012**, p. 239.
[133] J. Suikkola, T. Björninen, M. Mosallaei, T. Kankkunen, P. Iso-Ketola, L. Ukkonen, J. Vanhala, M. Mäntysalo, *Sci. Rep.* **2016**, *6*, 25784.
[134] P. Escobedo, M. A. Carvajal, L. F. Capitán-Vallvey, J. Fernández-Salmerón, A. Martínez-Olmos, A. J. Palma, *Sensors* **2016**, *16*, 1085.
[135] T. Leng, X. Huang, K. Chang, J. Chen, M. A. Abdalla, Z. Hu, *IEEE Antennas Wireless Propag. Lett.* **2016**, *15*, 1565.
[136] J. F. Salmerón, F. Molina-Lopez, D. Briand, J. J. Ruan, A. Rivadeneyra, M. A. Carvajal, L. F. Capitán-Vallvey, N. F. d. Rooij, A. J. Palma, *J. Electron. Mater.* **2014**, *43*, 604.
[137] J. Fernández-Salmerón, A. Rivadeneyra, F. Martínez-Martí, L. F. Capitán-Vallvey, A. J. Palma, M. A. Carvajal, *Sensors* **2015**, *15*, 26769.
[138] X. Huang, T. Leng, M. Zhu, X. Zhang, J. Chen, K. Chang, M. Aqeeli, A. K. Geim, K. S. Novoselov, Z. Hu, *Sci. Rep.* **2016**, *5*, 18298.
[139] R. Zichner, R. R. Baumann, *Jpn. J. Appl. Phys.* **2013**, *52*, 05DC24.
[140] J. Virkki, Z. Wei, A. Liu, L. Ukkonen, T. Björninen, *Int. J. Antennas Propag.* **2017**, *2017*, 3476017.
[141] M. A. Aziz, S. Roy, L. A. Berge, S. Nariyal, B. D. Braaten, in *2012 6th European Conf. on Antennas and Propagation (EUCAP)*, IEEE, Piscatawy, NJ, USA **2012**, p. 159.
[142] M. A. Ziai, J. C. Batchelor, *IEEE Trans. Antennas Propag.* **2011**, *59*, 3565.
[143] M. A. Ziai, J. C. Batchelor, *Proc. 5th European Conf. on Antennas and Propagation (EUCAP)*, IEEE, Piscataway, NJ, USA **2011**, p. 3811.
[144] D. E. Anagnostou, A. A. Gheethan, A. K. Amert, K. W. Whites, *J. Display Technol.* **2010**, *6*, 558.
[145] S. Beeby, Y. Li, J. Tudor, R. Torah, *Electron. Lett.* **2015**, *51*, 1306.
[146] R. Vyas, V. Lakafosis, A. Rida, N. Chaisilwattana, S. Travis, J. Pan, M. M. Tentzeris, *IEEE Trans. Microwave Theory Tech.* **2009**, *57*, 1370.
[147] M. Y. Chen, D. Pham, H. Subbaraman, X. Lu, R. T. Chen, *IEEE Trans. Microwave Theory Tech.* **2012**, *60*, 179.
[148] A. Martínez-Olmos, J. Fernández-Salmerón, N. Lopez-Ruiz, A. R. Torres, L. F. Capitan-Vallvey, A. J. Palma, *Anal. Chem.* **2013**, *85*, 11098.
[149] M. Jung, J. Kim, J. Noh, N. Lim, C. Lim, G. Lee, J. Kim, H. Kang, K. Jung, A. D. Leonard, J. M. Tour, G. Cho, *IEEE Trans. Electron Devices* **2010**, *57*, 571.
[150] H. Kang, H. Park, Y. Park, M. Jung, B. C. Kim, G. Wallace, G. Cho, *Sci. Rep.* **2015**, *4*, 5387.
[151] Y. Jung, H. Park, J.-A. Park, J. Noh, Y. Choi, M. Jung, K. Jung, M. Pyo, K. Chen, A. Javey, G. Cho, *Sci. Rep.* **2015**, *5*, 8105.
[152] M. Allen, C. Lee, B. Ahn, T. Kololuoma, K. Shin, S. Ko, *Microelectron. Eng.* **2011**, *88*, 3293.
[153] M. L. Allen, K. Jaakkola, K. Nummila, H. Seppä, *IEEE Trans. Compon. Packag. Technol.* **2009**, *32*, 325.
[154] A. Chiolerio, G. Maccioni, P. Martino, M. Cotto, P. Pandolfi, P. Rivolo, S. Ferrero, L. Scaltrito, *Microelectron. Eng.* **2011**, *88*, 2481.
[155] I. Ortego, N. Sanchez, J. Garcia, F. Casado, D. Valderas, J. I. Sancho, *Int. J. Antennas Propag.* **2012**, *2012*, 486565.
[156] W. Pachler, J. Grosinger, W. Bosch, G. Holweg, K. Popovic, A. Blumel, E. J. List-Kratochvil, in *2014 Loughborough Antennas and Propagation Conf. (LAPC)*, IEEE, Piscataway, NJ, USA **2014**, pp. 95–99.
[157] H. Park, H. Kang, Y. Lee, Y. Park, J. Noh, G. Cho, *Nanotechnology* **2012**, *23*, 344006.
[158] C.-H. Yang, J.-H. Chien, B.-Y. Wang, P.-H. Chen, D.-S. Lee, *Biomed. Microdevices* **2008**, *10*, 47.
[159] E. Abad, S. Zampolli, S. Marco, A. Scorzoni, B. Mazzolai, A. Juarros, D. Gómez, I. Elmi, G. C. Cardinali, J. M. Gómez,

© 2019 WILEY-VCH Verlag GmbH & Co. KGaA, Weinheim

F. Palacio, M. Cicioni, A. Mondini, T. Becker, I. Sayhan, *Sens. Actuators, B* **2007**, *127*, 2.
[160] H. Huang, *IEEE Sens. J.* **2013**, *13*, 3865.
[161] J. So, J. Thelen, A. Qusba, G. J. Hayes, G. Lazzi, M. D. Dickey, *Adv. Funct. Mater.* **2009**, *19*, 3632.
[162] S. Nikolaou, M. M. Tentzeris, J. Papapolymerou, in *2007 IEEE 18th Int. Symp. on Personal, Indoor and Mobile Radio Communications*, IEEE, Piscataway, NJ, USA **2007**, pp. 1–4, https://doi.org/10.1109/PIMRC.2007.4394348.
[163] A. Lazaro, R. Villarino, D. Girbau, *Sensors* **2018**, *18*, 3746.
[164] S.-E. Adami, D. Zhu, Y. Li, E. Mellios, B. H. Stark, S. Beeby, in *2015 IEEE Wireless Power Transfer Conference (WPTC)*, IEEE, Piscataway, NJ, USA **2015**, pp. 1–4, https://doi.org/10.1109/WPT.2015.7140161.
[165] S. Yang, J. Kim, *IET Microwaves, Antennas Propag.* **2012**, *6*, 756.
[166] D. Collins, *J. Power Sources* **1986**, *17*, 379.
[167] A. M. Gaikwad, A. C. Arias, D. A. Steingart, *Energy Technol.* **2015**, *3*, 305.
[168] S.-H. Kim, K.-H. Choi, S.-J. Cho, S. Choi, S. Park, S.-Y. Lee, *Nano Lett.* **2015**, *15*, 5168.
[169] S. Berchmans, A. J. Bandodkar, W. Jia, J. Ramírez, Y. S. Meng, J. Wang, *J. Mater. Chem. A* **2014**, *2*, 15788.
[170] M. Koo, K.-I. Park, S. H. Lee, M. Suh, D. Y. Jeon, J. W. Choi, K. Kang, K. J. Lee, *Nano Lett.* **2012**, *12*, 4810.
[171] K. Braam, V. Subramanian, *Adv. Mater.* **2015**, *27*, 689.
[172] M. Van Bavel, V. Leonov, R. F. Yazicioglu, T. Torfs, C. Van Hoof, N. Posthuma, R. Vullers, *Sens. Transducers J.* **2008**, *94*, 103.
[173] A. M. Gaikwad, A. M. Zamarayeva, J. Rousseau, H. Chu, I. Derin, D. A. Steingart, *Adv. Mater.* **2012**, *24*, 5071.
[174] A. M. Gaikwad, H. N. Chu, R. Qeraj, A. M. Zamarayeva, D. A. Steingart, *Energy Technol.* **2013**, *1*, 177.
[175] H. Gwon, J. Hong, H. Kim, D.-H. Seo, S. Jeon, K. Kang, *Energy Environ. Sci.* **2014**, *7*, 538.
[176] S. Xu, Y. Zhang, J. Cho, J. Lee, X. Huang, L. Jia, J. A. Fan, Y. Su, J. Su, H. Zhang, *Nat. Commun.* **2013**, *4*, 1543.
[177] Y. H. Kwon, S.-W. Woo, H.-R. Jung, H. K. Yu, K. Kim, B. H. Oh, S. Ahn, S.-Y. Lee, S.-W. Song, J. Cho, *Adv. Mater.* **2012**, *24*, 5192.
[178] N. Singh, C. Galande, A. Miranda, A. Mathkar, W. Gao, A. L. M. Reddy, A. Vlad, P. M. Ajayan, *Sci. Rep.* **2012**, *2*, 481.
[179] A. E. Ostfeld, A. M. Gaikwad, Y. Khan, A. C. Arias, *Sci. Rep.* **2016**, *6*, 26122.
[180] A. M. Zamarayeva, A. E. Ostfeld, M. Wang, J. K. Duey, I. Deckman, B. P. Lechêne, G. Davies, D. A. Steingart, A. C. Arias, *Sci. Adv.* **2017**, *3*, e1602051.
[181] M. Kaltenbrunner, G. Kettlgruber, C. Siket, R. Schwödiauer, S. Bauer, *Adv. Mater.* **2010**, *22*, 2065.
[182] X. Cao, C. Lau, Y. Liu, F. Wu, H. Gui, Q. Liu, Y. Ma, H. Wan, M. R. Amer, C. Zhou, *ACS Nano* **2016**, *10*, 9816.
[183] T. Yokota, P. Zalar, M. Kaltenbrunner, H. Jinno, N. Matsuhisa, H. Kitanosako, Y. Tachibana, W. Yukita, M. Koizumi, T. Someya, *Sci. Adv.* **2016**, *2*, e1501856.
[184] J. Kim, H. J. Shim, J. Yang, M. K. Choi, D. C. Kim, J. Kim, T. Hyeon, D. Kim, *Adv. Mater.* **2017**, *29*, 1700217.
[185] S. Park, S. W. Heo, W. Lee, D. Inoue, Z. Jiang, K. Yu, H. Jinno, D. Hashizume, M. Sekino, T. Yokota, *Nature* **2018**, *561*, 516.
[186] J. Chen, W. Cranton, M. Fihn, *Handbook of Visual Display Technology*, Springer, Berlin/Heidelberg, Germany **2016**.
[187] H. Jeong, L. Wang, T. Ha, R. Mitbander, X. Yang, Z. Dai, S. Qiao, L. Shen, N. Sun, N. Lu, *Adv. Mater. Technol.* **2019**, *4*, 1900117.
[188] H. U. Chung, B. H. Kim, J. Y. Lee, J. Lee, Z. Xie, E. M. Ibler, K. Lee, A. Banks, J. Y. Jeong, J. Kim, *Science* **2019**, *363*, eaau0780.
[189] W. Gao, S. Emaminejad, H. Y. Y. Nyein, S. Challa, K. Chen, A. Peck, H. M. Fahad, H. Ota, H. Shiraki, D. Kiriya, D.-H. Lien, G. A. Brooks, R. W. Davis, A. Javey, *Nature* **2016**, *529*, 509.
[190] D. P. Rose, M. E. Ratterman, D. K. Griffin, L. Hou, N. Kelley-Loughnane, R. R. Naik, J. A. Hagen, I. Papautsky, J. C. Heikenfeld, *IEEE Trans. Biomed. Eng.* **2014**, *62*, 1457.
[191] J. Kim, S. Imani, W. R. de Araujo, J. Warchall, G. Valdés-Ramírez, T. R. Paixão, P. P. Mercier, J. Wang, *Biosens. Bioelectron.* **2015**, *74*, 1061.
[192] Y. Khan, D. Han, A. Pierre, J. Ting, X. Wang, C. M. Lochner, G. Bovo, N. Yaacobi-Gross, C. Newsome, R. Wilson, *Proc. Natl. Acad. Sci. USA* **2018**, *115*, E11015.
[193] P. Mostafalu, A. Tamayol, R. Rahimi, M. Ochoa, A. Khalilpour, G. Kiaee, I. K. Yazdi, S. Bagherifard, M. R. Dokmeci, B. Ziaie, *Small* **2018**, *14*, 1703509.
[194] S. L. Swisher, M. C. Lin, A. Liao, E. J. Leeflang, Y. Khan, F. J. Pavinatto, K. Mann, A. Naujokas, D. Young, S. Roy, *Nat. Commun.* **2015**, *6*, 6575.
[195] A. Liao, M. C. Lin, L. C. Ritz, S. L. Swisher, D. Ni, K. Mann, Y. Khan, S. Roy, M. R. Harrison, A. C. Arias, V. Subramanian, D. Young, M. M. Maharbiz, in *2015 37th Annual Int. Conf. of the IEEE Engineering in Medicine and Biology Society (EMBC)*, IEEE, Piscataway, NJ, USA **2015**, pp. 5130–5133.
[196] S. Emaminejad, W. Gao, E. Wu, Z. A. Davies, H. Y. Y. Nyein, S. Challa, S. P. Ryan, H. M. Fahad, K. Chen, Z. Shahpar, *Proc. Natl. Acad. Sci. USA* **2017**, *114*, 4625.
[197] H. Y. Y. Nyein, L.-C. Tai, Q. P. Ngo, M. Chao, G. B. Zhang, W. Gao, M. Bariya, J. Bullock, H. Kim, H. M. Fahad, *ACS Sens.* **2018**, *3*, 944.
[198] J. Courbat, Y. Kim, D. Briand, N. De Rooij, in *2011 16th Int. Solid-State Sensors, Actuators and Microsystems Conf.*, IEEE, Piscataway, NJ, USA **2011**, pp. 1356–1359.
[199] A. V. Quintero, F. Molina-Lopez, G. Mattana, D. Briand, N. De Rooij, in *2013 Transducers & Eurosensors XXVII: The 17th Int. Conf. on Solid-State Sensors, Actuators and Microsystems (Transducers & Eurosensors XXVII)*, IEEE, Piscataway, NJ, USA **2013**, pp. 838–841.
[200] N.-B. Cho, T.-H. Lim, Y.-M. Jeon, M.-S. Gong, *Sens. Actuators, B* **2008**, *130*, 594.
[201] P. Escobedo, M. Erenas, N. Lopez-Ruiz, M. Carvajal, S. Gonzalez-Chocano, I. de Orbe-Paya, L. Capitan-Valley, A. Palma, A. Martinez-Olmos, *Anal. Chem.* **2017**, *89*, 1697.
[202] J. Gao, J. Sidén, H.-E. Nilsson, M. Gulliksson, *IEEE Sens. J.* **2013**, *13*, 1824.
[203] C.-W. Lee, D.-H. Nam, Y.-S. Han, K.-C. Chung, M.-S. Gong, *Sens. Actuators, B* **2005**, *109*, 334.
[204] F. Molina-Lopez, D. Briand, N. F. de Rooij, M. Smolander, in *SENSORS, 2012 IEEE*, IEEE, Piscataway, NJ, USA **2012**, pp. 1–4, https://doi.org/10.1109/ICSENS.2012.6411148.
[205] T. Unander, H.-E. Nilsson, *IEEE Sens. J.* **2009**, *9*, 922.
[206] T. Unander, J. Siden, H.-E. Nilsson, *IEEE Sens. J.* **2011**, *11*, 3009.
[207] J. Virtanen, L. Ukkonen, T. Bjorninen, A. Z. Elsherbeni, L. Sydänheimo, *IEEE Trans. Instrum. Meas.* **2011**, *60*, 2768.
[208] N. Clark, L. Maher, *React. Funct. Polym.* **2009**, *69*, 594.
[209] K. Crowley, A. Morrin, A. Hernandez, E. O'Malley, P. G. Whitten, G. G. Wallace, M. R. Smyth, A. J. Killard, *Talanta* **2008**, *77*, 710.
[210] V. Dua, S. P. Surwade, S. Ammu, S. R. Agnihotra, S. Jain, K. E. Roberts, S. Park, R. S. Ruoff, S. K. Manohar, *Angew. Chem., Int. Ed.* **2010**, *49*, 2154.
[211] A. Morata, J.-P. Viricelle, A. Tarancon, G. Dezanneau, C. Pijolat, F. Peiro, J. Morante, *Sens. Actuators, B* **2008**, *130*, 561.
[212] C. Castille, I. Dufour, M. Maglione, H. Debéda, C. Pellet, C. Lucat, *Procedia Chem.* **2009**, *1*, 971.
[213] A. Arena, N. Donato, G. Saitta, A. Bonavita, G. Rizzo, G. Neri, *Sens. Actuators, B* **2010**, *145*, 488.
[214] G. I. Hay, D. J. Southee, P. S. Evans, D. J. Harrison, G. Simpson, B. J. Ramsey, *Sens. Actuators, A* **2007**, *135*, 534.

© 2019 WILEY-VCH Verlag GmbH & Co. KGaA, Weinheim

[215] S. Merilampi, T. Björninen, L. Ukkonen, P. Ruuskanen, L. Sydänheimo, *Sens. Rev.* **2011**, *31*, 32.
[216] Y. Zhao, S. Gao, J. Zhu, J. Li, H. Xu, K. Xu, H. Cheng, X. Huang, *ACS Omega* **2019**, *4*, 9522.
[217] W. Tang, T. Yan, J. Ping, J. Wu, Y. Ying, *Adv. Mater. Technol.* **2017**, *2*, 1700021.
[218] S. Oren, H. Ceylan, P. S. Schnable, L. Dong, *Adv. Mater. Technol.* **2017**, *2*, 1700223.
[219] H.-N. Li, D.-S. Li, G.-B. Song, *Eng. Struct.* **2004**, *26*, 1647.
[220] H. Lee, K. M. Mosalam, *Earthquake Eng. Struct. Dyn.* **2014**, *43*, 317.
[221] M. Modares, N. Waksmanski, *Pract. Period. Struct. Des. Constr.* **2013**, *18*, 187.
[222] C. R. Farrar, K. Worden, *Structural Health Monitoring.: A Machine Learning Perspective*, John Wiley & Sons, Chichester, UK **2012**.
[223] J. Ko, Y. Ni, *Eng. Struct.* **2005**, *27*, 1715.
[224] X. Hu, B. Wang, H. Ji, *Comput.-Aided Civil Infrastructure Eng.* **2013**, *28*, 193.
[225] S. Kim, S. Pakzad, D. Culler, J. Demmel, G. Fenves, S. Glaser, M. Turon, in *IPSN '07 Proc. of the 6th Int. Conf. on Information Processing in Sensor Networks*, Association for Computing Machinery (ACM), New York **2007**, pp. 254–263.
[226] D. Huston, *Structural Sensing, Health Monitoring, and Performance Evaluation*, CRC Press, Boca Raton, FL, USA **2010**.
[227] R. C. Tennyson, A. A. Mufti, S. Rizkalla, G. Tadros, B. Benmokrane, *Smart Mater. Struct.* **2001**, *10*, 560.
[228] T.-H. Yi, H.-N. Li, M. Gu, *Measurement* **2013**, *46*, 420.
[229] D. Feng, M. Feng, E. Ozer, Y. Fukuda, *Sensors* **2015**, *15*, 16557.
[230] Z.-S. Guo, *Struct. Health Monit.: Int. J.* **2007**, *6*, 191.
[231] S. Bagavathiappan, B. Lahiri, T. Saravanan, J. Philip, T. Jayakumar, *Infrared Phys. Technol.* **2013**, *60*, 35.
[232] J. Ou, H. Li, *Struct. Health Monit.: Int. J.* **2010**, *9*, 219.
[233] G. S. Duffó, S. B. Farina, *Constr. Build. Mater.* **2009**, *23*, 2746.
[234] A. Nair, C. Cai, *Eng. Struct.* **2010**, *32*, 1704.
[235] V. G. M. Annamdas, S. Bhalla, C. K. Soh, *Struct. Health Monit.: Int. J.* **2017**, *16*, 324.
[236] J. M. W. Brownjohn, *Philos. Trans. R. Soc., A* **2007**, *365*, 589.
[237] S. W. Doebling, C. R. Farrar, M. B. Prime, *Shock Vib. Dig.* **1998**, *30*, 91.
[238] R. O. Hamburger, *A Policy Guide to Steel Moment-Frame Construction*, SAC Joint Venture **2000**.
[239] J. P. Lynch, *Shock Vib. Digest* **2006**, *38*, 91.
[240] D. Zymelka, T. Yamashita, S. Takamatsu, T. Itoh, T. Kobayashi, *Sens. Actuators, A* **2017**, *263*, 391.
[241] M. I. Todorovska, M. D. Trifunac, *Soil Dyn. Earthquake Eng.* **2007**, *27*, 564.
[242] C. R. Farrar, W. E. Baker, T. M. Bell, K. M. Cone, T. W. Darling, T. A. Duffey, A. Eklund, A. Migliori, **2005**.
[243] S. Dorvash, S. N. Pakzad, E. L. LaCrosse, J. M. Ricles, I. C. Hodgson, *Earthquake Spectra* **2015**, *31*, 1543.
[244] M. I. Todorovska, M. D. Trifunac, *Struct. Control Health Monit.* **2008**, *15*, 90.
[245] S. Muin, K. M. Mosalam, *Earthquake Spectra* **2017**, *33*, 641.
[246] C. Loh, C. Chan, S. Chen, S. Huang, *Earthquake Eng. Struct. Dyn.* **2016**, *45*, 699.
[247] T. Chan, L. Yu, H. Tam, Y. Ni, S. Liu, W. Chung, L. Cheng, *Eng. Struct.* **2006**, *28*, 648.
[248] K. Wong, *Struct. Control Health Monit.* **2004**, *11*, 91.
[249] T.-C. Hou, K. J. Loh, J. P. Lynch, *Nanotechnology* **2007**, *18*, 315501.
[250] K. J. Loh, T.-C. Hou, J. P. Lynch, N. A. Kotov, *J. Nondestr. Eval.* **2009**, *28*, 9.
[251] R. Zhang, H. Deng, R. Valenca, J. Jin, Q. Fu, E. Bilotti, T. Peijs, *Compos. Sci. Technol.* **2013**, *74*, 1.
[252] D. Ryu, F. N. Meyers, K. J. Loh, *J. Intell. Mater. Syst. Struct.* **2015**, *26*, 1699.
[253] F. N. Meyers, K. J. Loh, J. S. Dodds, A. Baltazar, *Nanotechnology* **2013**, *24*, 185501.
[254] N. Salowitz, Z. Guo, Y.-H. Li, K. Kim, G. Lanzara, F.-K. Chang, *J. Compos. Mater.* **2013**, *47*, 97.
[255] F. Kopsaftopoulos, R. Nardari, Y.-H. Li, F.-K. Chang, *Mech. Syst. Signal Process.* **2018**, *98*, 425.
[256] X. Chen, T. Topac, W. Smith, P. Ladpli, C. Liu, F.-K. Chang, *Sensors* **2018**, *18*, 3260.
[257] Y. Xu, F. Jiang, S. Newbern, A. Huang, C.-M. Ho, Y.-C. Tai, *Sens. Actuators, A* **2003**, *105*, 321.
[258] Y. Zhang, N. Anderson, S. Bland, S. Nutt, G. Jursich, S. Joshi, *Sens. Actuators, A* **2017**, *253*, 165.
[259] G.-Y. Lee, M.-S. Kim, H.-S. Yoon, J. Yang, J.-B. Ihn, S.-H. Ahn, *Proc. CIRP* **2017**, *66*, 238.
[260] Y. Zhao, M. Schagerl, S. Gschossmann, C. Kralovec, *Struct. Health Monit.* **2019**, *18*, 1479.
[261] J. Y. Oh, Z. Bao, *Adv. Sci.* **2019**, *6*, 1900186.
[262] J. Zhou, T. Ge, E. Ng, J. S. Chang, *IEEE Trans. Electron Devices* **2015**, *63*, 793.
[263] S. Sivapurapu, R. Chen, C. Mehta, Y. Zhou, M. L. Bellaredj, X. Jia, P. Kohl, T.-C. Huang, S. K. Sitaraman, M. Swaminathan, *IEEE Trans. Compon., Packag. Manuf. Technol.* **2019**, https://doi.org/10.1109/TCPMT.2019.2931452.

 © 2019 WILEY-VCH Verlag GmbH & Co. KGaA, Weinheim